Direct and indirect capture of near-Earth asteroids in the Earth-Moon system

Minghu Tan

School of Engineering
University of Glasgow, Glasgow G12 8QQ, UK
m.tan.2@research.gla.ac.uk
Phone: ++44 (0)756 108 7644

Colin McInnes

School of Engineering
University of Glasgow, Glasgow G12 8QQ, UK
Colin.McInnes@glasgow.ac.uk
Phone: ++44 (0)141 330 8511

Matteo Ceriotti

School of Engineering
University of Glasgow, Glasgow G12 8QQ, UK
Matteo.Ceriotti@glasgow.ac.uk
Phone: +44 (0)141 330 6465

Abstract

Near-Earth asteroids have attracted attention for both scientific and commercial mission applications. Due to the fact that the Earth-Moon L_1 and L_2 points are candidates for gateway stations for lunar exploration, and an ideal location for space science, capturing asteroids and inserting them into periodic orbits around these points is of significant interest for the future. In this paper, we define a new type of lunar asteroid capture, termed direct capture. In this capture strategy, the candidate asteroid leaves its heliocentric orbit after an initial impulse, with its dynamics modelled using the Sun-Earth-Moon restricted four-body problem until its insertion, with a second impulse, onto the L_2 stable manifold in the Earth-Moon circular restricted three-body problem. A Lambert arc in the Sun-asteroid two-body problem is used as an initial guess and a differential corrector used to generate the transfer trajectory from the asteroid's initial obit to the stable manifold associated with Earth-Moon L_2 point. Results show that the direct asteroid capture strategy needs a shorter flight time compared to an indirect asteroid capture, which couples capture in the Sun-Earth circular restricted three-body problem and subsequent transfer to the Earth-Moon

circular restricted three-body problem. Finally, the direct and indirect asteroid capture strategies are also applied to consider capture of asteroids at the triangular libration points in the Earth-Moon system.

Keywords: Circular restricted three-body problem, periodic orbits, stable manifolds, direct asteroid capture, indirect asteroid capture

1 Introduction

As a focus for new research, near-Earth Asteroids (NEAs) have attracted significant attention for scientific mission applications (Zimmer 2013; Hasnain et al. 2012; Brophy et al. 2012b). Moreover, there is a growing commercial interest in NEA resources (Tronchetti 2014; Andrews et al. 2015). While they may make close approaches to the Earth and represent a potential impact threat, NEAs can provide opportunities to exploit in-situ resources for future space exploration.

The idea of capturing small NEAs with relatively low energy has been investigated in detail in recent work (Sanchez and McInnes 2011; Hasnain et al. 2012; Sanchez et al. 2012). In these studies, periodic orbits around the Sun-Earth L_1 and L_2 libration points are regarded as potential parking orbits for captured asteroids, since the Sun-Earth L_1 and L_2 points are natural gateways to other systems, e.g., the Earth-Moon (EM) system (Koon et al. 2000). Among those small NEAs, a new class of NEAs, termed the Easily Retrievable Objects (EROs) was proposed by Yárnoz et al. (2013). These are NEAs which can be captured into periodic orbits around the L_1 and L_2 libration points in the Sun–Earth circular restricted three-body problem (CRTBP) with the total Δv cost below 500 ms^{-1}. Moreover, Ceriotti and Sanchez (2016) proposed a strategy to control such EROs retrieval trajectories to solve the problems caused by uncertainties in asteroid mass and injection maneuvers.

Periodic orbits around the libration points and the invariant manifolds associated with them have generated significant interest in NEAs exploration missions, including the NEA flyby (Gao 2013), NEA capture (Yárnoz et al. 2013) and the spacecraft reusability for NEA exploration (Zimmer 2013). Moreover, periodic orbits with unstable characteristics can be utilized to design low-energy ballistic transfers (Lo and Parker 2004; Davis et al. 2011). Again, these orbits can also serve as parking orbits for captured NEAs (Sanchez et al. 2012; Mingotti et

al. 2014a). Meanwhile, invariant manifolds have been utilized as the basic mathematical tool to design low-energy transfer trajectories between different multi-body systems, e.g., the Earth–Moon and Sun–Earth systems (Koon et al. 2000; Koon et al. 2011; Howell and Kakoi 2006). During such transfers, the spacecraft or the candidate NEA should first be inserted onto the stable manifold associated with the target periodic orbit around the libration point of interest. Once inserted onto the stable manifold, it will be asymptotically captured without further active maneuvers. A successful application of this method is to the design of the Hiten-like mission trajectory (Koon et al. 2001). A further example of trajectory design includes transfer between libration point orbits (LPOs) within a restricted three-body system and transfer trajectories in multi-body dynamical systems (Qi and Xu 2016). Missions including Genesis, WMAP, Triana, ISEE-3 and WIND have utilized the circular restricted three-body problem to design transfers to and from LPOs in the Sun-Earth system. Moreover, the patched circular restricted three-body problem was introduced by Koon et al. (2000) and has been used to design low-energy transfer trajectories from the Earth to the Moon (Koon et al. 2000; Koon et al. 2001; de Sousa-Silva and Terra 2016). Based on the patched restricted three-body problem approximation, the bi-circular restricted four-body model was proposed to design the low-cost Earth-Moon transfer trajectories (Koon et al. 2011; Topputo 2013).

Based on ballistic capture mechanics in the restricted three-body problem, transfers between NEAs and LPOs have also been investigated in recent years (Yárnoz et al. 2013; Mingotti et al. 2014a; Farquhar et al. 2004; Zimmer 2013; Wang et al. 2013; Gao 2013). For example, Mingotti et al. (2014a) proposed the use of low thrust propulsion to capture NEAs to a target periodic orbit around the Sun-Earth L_1 and L_2 points by using the stable manifolds associated with the target periodic orbit. Farquhar et al. (2004) regard the Sun–Earth L_2 libration point as a potential parking orbit and gateway station for missions to NEAs and Mars. Delivering NEA resources to a LPO at the L_2 point could therefore provide efficient logistic support. In order to lower the cost of space exploration missions, Zimmer (2013) studied reusability by stationing spacecraft on periodic orbits at the Sun–Earth L_1 and L_2 points between NEA missions. In related work, a differential correction method was proposed to design flyby trajectories from a

Lissajous orbit of the CHANG'E 2 spacecraft to the asteroids Toutatis and 2010 JK1 (Wang et al. 2013).

The Earth–Moon libration points are also key to the future of deep space exploration. In 2010, the two ARTEMIS spacecraft became the first vehicles to operate in the vicinity of an Earth-Moon libration point, operating successfully in this dynamical regime from August 2010 through July 2011 (Folta et al. 2011). In 2011, NASA released a report on Earth-Moon libration point missions as part of 'The Global Exploration Roadmap' (Hufenbach et al. 2011). NASA has identified the Earth-Moon L_1 and L_2 points as potential locations of interest for future human space exploration (Olson 2012). Meanwhile, NASA has also proposed a potential future mission, the Near-Earth Asteroid Redirect Mission (ARM), to rendezvous with and then capture a small near-Earth asteroid (later a boulder from a near-Earth asteroid) (Brophy et al. 2012a). Given that final placement of the captured asteroid in the vicinity of the Earth may incur an impact risk, it is prudent to place the retrieved asteroid in an orbit from which it could only impact the Moon. Lunar orbits, or possibly regions near the Earth-Moon Lagrange points, would therefore be one of preferred locations, although there is additional work required on this matter. Besides, the Earth-Moon L_2 point is also regarded as a candidate gateway for future space missions, since spacecraft on periodic orbits around the Earth-Moon L_2 point can easily achieve low-energy transfers to the vicinity of the Moon and the vicinity of the Sun–Earth L_1 and L_2 points (Lo and Ross 2001; Alessi et al. 2009; Davis et al. 2010). Therefore, capturing asteroids and inserting them directly at the Earth-Moon L_1 and L_2 points may be of significant benefit for future space exploration by providing in-situ resources. In addition, due to the fact the triangular points in the Earth-Moon system are stable, the propellant required to maintain a captured NEA at such a location is modest (Salazar et al. 2012). For this reason, it may also be of interest to capture an NEA and place it on a periodic orbit around the triangular L_4 and L_5 points in the Earth-Moon system. Furthermore, due to fact that the Earth-Moon L_4 and L_5 points can be used as a parking orbit for travel to and from cislunar space, O'Neill (1974) proposed to build space colonies at these points where captured NEAs could provide material for these large structures. Accordingly, DeFilippi Jr (1977) studied station-keeping strategies at Earth-Moon L_4 point.

Mingotti et al. (2014b) proposed the patched circular restricted three-body

problem as a model, which consists of the Sun–Earth and the Earth–Moon CRTBP systems, to capture NEAs onto target periodic orbits around the Earth–Moon L_2 point. However, this would require a significant duration for the asteroid to be asymptotically captured onto periodic orbits around the Sun-Earth L_1 or L_2 points, compared to the traditional hyperbolic approach (Sanchez et al. 2012). For this reason, we propose a new type of lunar asteroid capture, termed direct capture. In this capture strategy, an initial impulse will modify the asteroid's orbit and a second impulse will insert it onto the stable manifold associated with the Earth-Moon L_2 periodic orbits directly. Then, the asteroid will be asymptotically captured onto the target periodic orbit around the L_2 point in Earth-Moon system. The transfer trajectories from the asteroid's orbit to the stable manifold associated with the Earth-Moon L_2 periodic orbits are modelled by the Sun-Earth-Moon restricted four-body problem. It should be noted that the patched three-body problem is an approximation of the Sun-Earth-Moon four-body problem and it is decomposed into the Earth-Moon CRTBP and Sun-Earth CRTBP. The Sun-Earth-Moon restricted four-body problem incorporates the perturbation of the Moon into the Sun-Earth CRTBP.

In this paper, the CRTBP is used to compute the stable manifolds associated with periodic orbits in the Earth-Moon system and then the Moon-Sun three-body sphere of influence (3BSOI) is utilized as the boundary between the Sun-Earth-Moon restricted four-body problem and the Earth-Moon CRTBP. Then the target points on the stable manifolds are transformed to the Sun-centered inertial frame. The three-dimensional orbital-element space of candidate NEAs is then obtained to select candidate NEAs which can be captured with a total cost under 500 ms^{-1}. After calculating the approximate approach date and departure date, a Lambert arc in the Sun-centered two-body problem is utilized to estimate the first impulse to the target points from the candidate asteroid's orbit. Based on the initial guess of the first impulse, a differential correction method is then used to design the transfer trajectory to the target points from the candidate asteroid's orbit in the Sun-Earth-Moon restricted four-body problem. Results show that the direct asteroid capture strategy needs a shorter flight time compared to an indirect asteroid capture, which couples together the Sun-Earth CRTBP and the Earth-Moon CRTBP.

The paper is organized as follows. Section 2 presents a set of dynamical models, including the Earth-Moon restricted three-body problem and the Sun-Earth-Moon restricted four-body problem; Section 3 considers periodic orbits (Lyapunov orbits and Halo orbits) around the Earth-Moon L_2 point and the stable manifolds associated with those periodic orbits; Section 4 proposes the concept of direct capture of NEAs in the Earth-Moon CRTBP and describes the detailed design procedure to calculate the transfer trajectory of an asteroid from its initial orbit to the stable manifolds associated with Earth-Moon L_2 periodic orbits; finally these results are optimized using the NSGA-II algorithm; Section 5 considers the calculation of the indirect capture of NEAs in the Earth-Moon system by using the patched restricted three-body problem model which consists of the Sun-Earth CRTBP system and Earth-Moon CRTBP system; Section 6 investigates the direct and indirect capture of NEAs to the triangular points in the Earth-Moon CRTBP system.

2 Dynamical models

2.1 Circular restricted three-body problem

To describe the motion of captured NEAs in the Earth-Moon system, the model of the circular restricted three-body problem (CRTBP) is adopted. Assuming that the Earth and Moon are in a circular orbit around their common center-of-mass, the motion of NEAs in the rotating frame, which is centered at the barycenter of the Earth and Moon system, is defined by

$$\begin{cases} \ddot{x} - 2\dot{y} = \dfrac{\partial \Omega}{\partial x} \\ \ddot{y} + 2\dot{x} = \dfrac{\partial \Omega}{\partial y} \\ \ddot{z} = \dfrac{\partial \Omega}{\partial z} \end{cases} \tag{1}$$

where

$$\Omega(x, y, z, \mu) = \frac{1}{2}[(x^2 + y^2) + \mu(1-\mu)] + \frac{1-\mu}{r_1} + \frac{\mu}{r_2}$$

and $r_1 = [(x+\mu)^2 + y^2 + z^2]^{1/2}$, $r_2 = [(x-1+\mu)^2 + y^2 + z^2]^{1/2}$ are the magnitudes of the position vectors to the Earth and Moon, scaled by the distance between the

Earth and Moon; μ is the non-dimensional mass ratio of the Earth and Moon. The coordinates of the Earth and Moon in the rotating frame are [$-\mu$, 0, 0] and [$1-\mu$, 0, 0], respectively, as shown in Fig. 1. The unit of time is chosen such that the orbital period of the Earth and Moon about their barycenter is 2π.

For the CRTBP, the Jacobi constant J is (Koon et al. 2011)

$$2\Omega(x, y, z, \mu) - (\dot{x}^2 + \dot{y}^2 + \dot{z}^2) = J \tag{2}$$

The five libration points, L_i, (i = 1, 2 . . . 5) can be obtained from Eq. (1), shown in Fig. 1. The mass parameter assumed for the Earth-Moon model is μ = 1.2155650×10^{-2}.

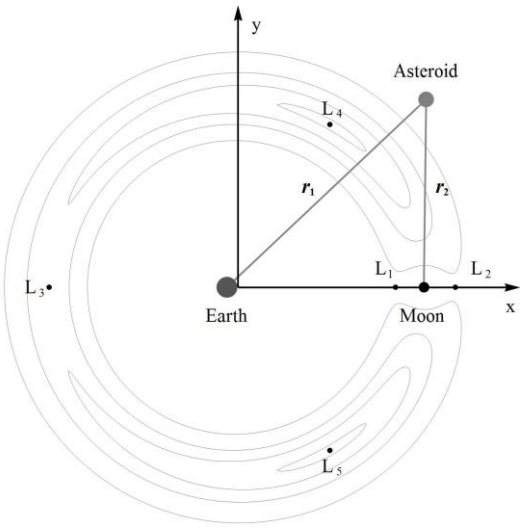

Fig. 1 Earth-Moon CRTBP with five libration points and Jacobi constant contours

2.2 Sun-Earth-Moon restricted four-body problem model

When designing transfer trajectories from the initial asteroid orbit to the stable manifolds in the Earth-Moon CRTBP system, we assume that the motion of the asteroid is governed by the gravity of the Sun, Earth and Moon. It is also assumed that the motion of Moon with respect to Earth and the motion of the Earth with respect to the Sun are described by the two-body problem. Here the Sun-centered inertial frame is used to describe the Sun-Earth-Moon restricted four-body system such that

$$\begin{cases} \ddot{\boldsymbol{r}} = -\dfrac{\mu_{Sun}}{r^3}\boldsymbol{r} - \dfrac{\mu_{Earth}}{r_{ea}^{\ 3}}(\boldsymbol{r}-\boldsymbol{r}_e) - \dfrac{\mu_{Moon}}{r_{ma}^{\ 3}}(\boldsymbol{r}-\boldsymbol{r}_e-\boldsymbol{r}_m) \\ \ddot{\boldsymbol{r}}_e = -\dfrac{\mu_{Sun}}{r_{es}^{\ 3}}\boldsymbol{r}_e \\ \ddot{\boldsymbol{r}}_m = -\dfrac{\mu_{Earth}}{r_{me}^{\ 3}}\boldsymbol{r}_m \end{cases} \tag{3}$$

where

$$r_{ea} = \|\boldsymbol{r}-\boldsymbol{r}_e\|, r_{ma} = \|\boldsymbol{r}-\boldsymbol{r}_e-\boldsymbol{r}_m\|, r_{es} = \|\boldsymbol{r}_e\|, r_{me} = \|\boldsymbol{r}_m\|$$

where $\boldsymbol{r}$ is the position vector of the asteroid with respect to the Sun; $\boldsymbol{r}_e$ is the position vector of the Earth with respect to the Sun in the two-body problem; $\boldsymbol{r}_m$ is the position vector of Moon with respect to the Earth in the two-body problem and it is initialized with a state of the Moon with respect to the Earth from the real ephemeris, shown in Fig. 2. The motion of all four bodies are assumed to be in the same plane. In addition, μ_{Sun}, μ_{Earth} and μ_{Moon} are the gravitational parameters of the Sun, Earth and Moon, respectively. The gravitational parameters assumed for this model are μ_{Sun}= 1.3271244×10^{11} km/s^2. μ_{Earth}= 3.9860044×10^5 km/s^2 and μ_{Moon}= 4.9048695×10^3 km/s^2.

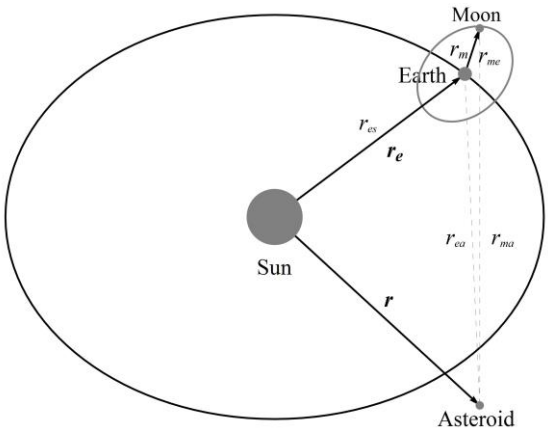

Fig. 2 Geometry of the Sun-Earth-Moon restricted four-body problem

3 Periodic orbits and invariant manifolds

3.1 Earth-Moon L_2 periodic orbits

Families of periodic orbits around the collinear libration points L_1 and L_2 in the CRTBP have been studied extensively (Richardson 1980; Gómez 2001). There

are two key classes of periodic orbits: halo orbits and Lyapunov orbits. The initial states of such periodic orbits can be computed by utilizing the differential correction method (Howell and Pernicka 1987), based on Richardson's third order approximation (Richardson 1980); we then follow this process by numerical continuation to generate a series of periodic orbits with increasing or decreasing Jacobi constant *J*, as shown in Fig. 3, where the unit of length is the Earth-Moon distance (EM unit).

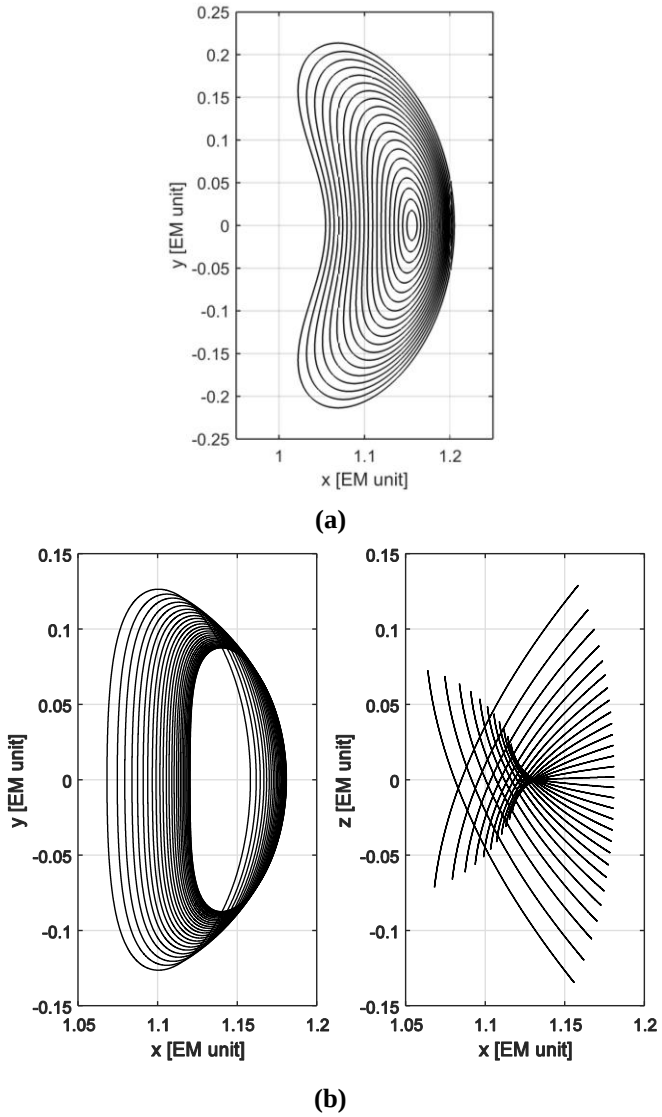

Fig. 3 (a) Planar Lyapunov orbits with Jacobi constant [2.99533289, 3.17205221] and (b) halo orbits with Jacobi constant [3.06733209, 3.15211497] around L_2 point in the Earth-Moon system.

3.2 Invariant manifolds

Invariant manifolds associated with periodic orbits around the collinear L_1 and L_2 libration points are trajectories which asymptotically approach or depart these target periodic orbits (Koon et al. 2011). The stable manifold W^S associated with a periodic orbit consists of all trajectories that reach this target periodic orbit along the periodic orbit's stable eigenvector. The unstable manifold W^U associated with a periodic orbit includes all possible trajectories that depart from this target orbit along the target orbit's unstable eigenvector. Therefore, the stable manifold in the CRTBP can be calculated by propagating backward from an initial condition as follows

$$\boldsymbol{X}_S = \boldsymbol{X}_0 \pm \varepsilon \boldsymbol{V}_S \tag{4}$$

and the unstable manifold can be computed by propagating forward from the following initial condition

$$\boldsymbol{X}_U = \boldsymbol{X}_0 \pm \varepsilon \boldsymbol{V}_U \tag{5}$$

where $\boldsymbol{V}_S / \boldsymbol{V}_U$ are the stable/unstable eigenvectors of the monodromy matrix evaluated at a point $\boldsymbol{X}_0 = [x_0, y_0, z_0, \dot{x}_0, \dot{y}_0, \dot{z}_0]^T$ on the periodic orbit. The parameter ε represents the magnitude of the perturbation, in the direction of the stable/unstable eigenvectors, between the periodic orbit and the initial condition of the stable/unstable manifolds. Gómez et al. (1991) suggests values of ε corresponding to non-dimensional position displacements of order 10^{-6} (corresponding to about 0.38km in the position and about 10^{-6} km/s in the velocity in the Earth-Moon system). We refer to the backward propagation time as the stable manifold transfer time t_{sm} and the forward propagation time as the unstable manifold transfer time t_{um}.

A Poincaré section can replace a continuous dynamical system with a discrete dynamical system. Here the Poincaré section is defined by the angle θ ($\theta > 0$), shown in Fig. 4.

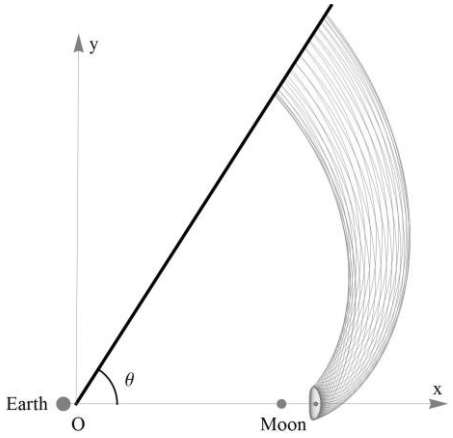

Fig. 4 Stable manifolds associated with Lyapunov orbits around the Earth-Moon L_2 point

Then, the stable manifolds on the Poincaré section in the Earth-Moon rotating system can be defined as

$$X_{EM}^{ro}(J,\theta)=\left\{(x,y,z,\dot{x},\dot{y},\dot{z})\in W^{S}\,\middle|\,y=(x+\mu)\tan\theta, 2\Omega(x,y,z,\mu)-(\dot{x}^2+\dot{y}^2+\dot{z}^2)=J\right\} \tag{6}$$

The superscript "*ro*" and the subscript "*EM*" in Eq. (6) denote the rotating frame and Earth-Moon system respectively.

3.3 Coordinate transformation

The position of the Moon in an Earth-centered inertial frame can be described by the angle β, shown in Fig. 5. It should be noticed that the angle We denote the states of the EM L_2 stable manifold in the Earth-Moon rotating frame and in the Earth-centered inertial frame by $\boldsymbol{X}_{EM}^{ro}$ and $\boldsymbol{X}_{E}^{in}$ respectively. Thus we have the transformation

$$\boldsymbol{X}_{E}^{in}=\boldsymbol{R}(\beta)(\boldsymbol{X}_{EM}^{ro}+[\mu,0,0,0,0,0]^{T}),\beta\in[0,2\pi] \tag{7}$$

where

$$\boldsymbol{R}(\beta)=\begin{bmatrix}\cos\beta & -\sin\beta & 0 & 0 & 0 & 0\\ \sin\beta & \cos\beta & 0 & 0 & 0 & 0\\ 0 & 0 & 1 & 0 & 0 & 0\\ -\sin\beta & -\cos\beta & 0 & \cos\beta & -\sin\beta & 0\\ \cos\beta & -\sin\beta & 0 & \sin\beta & \cos\beta & 0\\ 0 & 0 & 0 & 0 & 0 & 1\end{bmatrix}$$

and the state of the EM L_2 stable manifold in the Sun-centered inertial frame is then defined by

$$\boldsymbol{X}_S^{in} = \boldsymbol{X}_e + \boldsymbol{X}_E^{in} \tag{8}$$

where $\boldsymbol{X}_e = [\boldsymbol{r}_e; \dot{\boldsymbol{r}}_e]$

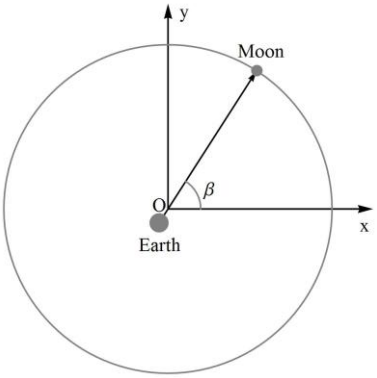

Fig. 5 Geometry of the Moon in the inertial frame which is centered at the barycenter of the Earth-Moon system

4 Direct capture of near-Earth asteroids in the Earth-Moon system

4.1 Concept of direct capture

The basic concept of direct capture of NEAs is through the following strategy:

(1) With an initial maneuver $\Delta\boldsymbol{v}_1$, the candidate asteroid leaves its orbit and is modelled in the Sun-Earth-Moon restricted four-body system, shown in Fig. 6(a);

(2) After a second maneuver $\Delta\boldsymbol{v}_2$, the candidate asteroid inserts onto the stable manifold associated with the periodic orbit around the EM L_2 point and will be asymptotically captured onto it, shown in Fig. 6(b).

The total cost of capturing the NEA onto the stable manifold associated with the periodic orbit around EM L_2 point is therefore calculated as

$$\Delta v = \left\|\Delta\boldsymbol{v}_1\right\| + \left\|\Delta\boldsymbol{v}_2\right\| \tag{9}$$

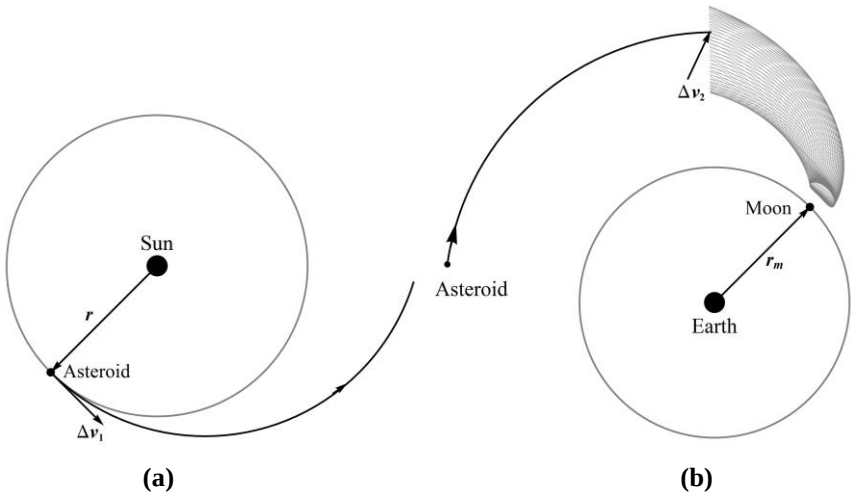

Fig. 6 Direct capture of near-Earth asteroid: (a) initial impulse Δv_1 for the asteroid to leave its orbit; (b) second impulse Δv_2 to insert the asteroid onto the stable manifold associated with the periodic orbit around the Earth-Moon L_2 point

Thus, for each candidate NEA, there are 5 variables to describe the sequence of maneuvers as follows:

- T_0: departure date when the first impulse $\Delta \boldsymbol{v}_1$ is applied to the candidate asteroid and the asteroid leaves its initial orbit;
- T_f: approach date corresponding to the date when the candidate asteroid inserts onto the EM L_2 stable manifold with the second impulse $\Delta \boldsymbol{v}_2$;
- J: Jacobi constant of the final periodic orbit around EM L_2;
- t_p: time determining the state on the target periodic orbit around EM L_2 where the EM L_2 stable manifold is propagated backward from; $t_p \in [0, T_p]$ where T_p is the period of the final periodic orbit;
- t_{sm}: stable manifold transfer time determining the target point where the second impulse is applied.

4.2 Differential correction

A heliocentric two-body Lambert arc with two impulsive maneuvers can be used to provide an initial guess, where the first impulse is applied and the asteroid transfers to the Earth-Moon system. It will be assumed that the initial state of the asteroid is $\boldsymbol{X}_i = [x_i, y_i, z_i, \dot{x}_i, \dot{y}_i, \dot{z}_i]^T$ after the first impulse, the state of the target point is $\boldsymbol{X}_f = [x_f, y_f, z_f, \dot{x}_f, \dot{y}_f, \dot{z}_f]^T$ and the final state of the Lambert arc is $\boldsymbol{X}_f^{'} = [x_f^{'}, y_f^{'}, z_f^{'}, \dot{x}_f^{'}, \dot{y}_f^{'}, \dot{z}_f^{'}]^T$, before the second impulse, as shown Fig. 7. Then we

can seek conditions for $\delta \boldsymbol{r_f} = [\delta x_f, \delta y_f, \delta z_f]^T = [x_f - x_f^{'}, y_f - y_f^{'}, z_f - z_f^{'}]^T = \mathbf{0}$ by correcting the initial velocity vector $\delta \boldsymbol{v_i} = [\delta \dot{x}_i, \delta \dot{y}_i, \delta \dot{z}_i]^T$.

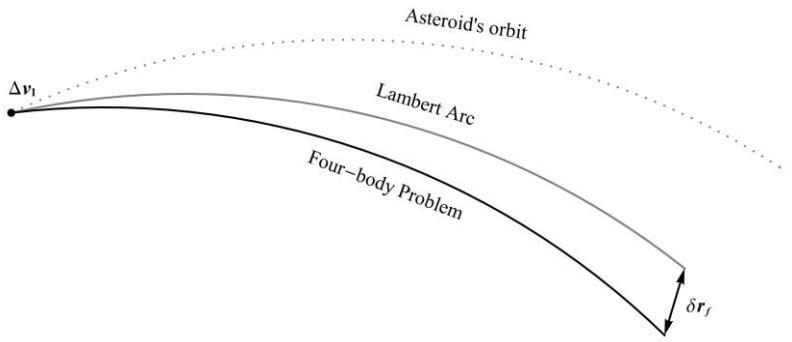

Fig. 7 Differential correction with an initial guess using a Lambert transfer

We assume that the Sun-Earth-Moon restricted four-body system in Eq. (3) can be represented by a set of nonlinear equations of motion in the general form

$$\dot{\boldsymbol{X}} = \boldsymbol{f}(\boldsymbol{X}, t) \tag{10}$$

where

$$\boldsymbol{X} = [x, y, z, \dot{x}, \dot{y}, \dot{z}]^T$$

We then label the solution $\boldsymbol{X}_0(t)$ as the reference trajectory of Eq. (10). Defining the relationship between the reference trajectory $\boldsymbol{X}_0(t)$ and a nearby trajectory $\boldsymbol{X}(t)$, as

$$\boldsymbol{X}(t) = \boldsymbol{X}_0(t) + \delta \boldsymbol{X}(t) \tag{11}$$

and expanding about the reference solution in a Taylor series generates a set of linear equations, such that

$$\delta \dot{\boldsymbol{X}} = \boldsymbol{A}(t) \delta \boldsymbol{X} \tag{12}$$

where $\boldsymbol{A}(t) = \left. \frac{\partial \boldsymbol{f}}{\partial \boldsymbol{X}} \right|_{\boldsymbol{X}_0}$. The general solution to the above equation is

$$\delta \boldsymbol{X}(t) = \Phi(t, t_0) \delta \boldsymbol{X}(t_0) \tag{13}$$

where the state transition matrix is found from

$$\dot{\Phi}(t, t_0) = \boldsymbol{A}(t) \Phi(t, t_0), \Phi(t_0, t_0) = \boldsymbol{I}$$

Then we can obtain

$$\boldsymbol{A}(t) = \frac{d\boldsymbol{f}(\boldsymbol{X}, t)}{d\boldsymbol{X}} = \begin{bmatrix} \mathbf{0} & \boldsymbol{I} \\ \Psi & \mathbf{0} \end{bmatrix} \tag{14}$$

where $\Psi = \begin{bmatrix} \frac{\partial \ddot{x}}{\partial x} & \frac{\partial \ddot{x}}{\partial y} & \frac{\partial \ddot{x}}{\partial z} \\ \frac{\partial \ddot{y}}{\partial x} & \frac{\partial \ddot{y}}{\partial y} & \frac{\partial \ddot{y}}{\partial z} \\ \frac{\partial \ddot{z}}{\partial x} & \frac{\partial \ddot{z}}{\partial y} & \frac{\partial \ddot{z}}{\partial z} \end{bmatrix}$

The differential correction can therefore be written as

$$\delta \boldsymbol{X}_{\boldsymbol{i}} = \Phi^{-1} \delta \boldsymbol{X}_{\boldsymbol{f}} \tag{15}$$

where $\delta \boldsymbol{X}_{\boldsymbol{i}} = [0,0,0,\delta \dot{x}_i, \delta \dot{y}_i, \delta \dot{z}_i]^T, \delta \boldsymbol{X}_{\boldsymbol{f}} = [\delta x_f, \delta y_f, \delta z_f, 0,0,0]^T$.

The differential correction in Eq. (15) starts with the initial state $\boldsymbol{X_0}$ which is based on the Lambert arc and then the process is repeated until $\delta \boldsymbol{r}_{\boldsymbol{f}} = [\delta x_f, \delta y_f, \delta z_f]^T$ is equal to **0** within some small tolerance.

4.3 Target point filter

After the first impulse, the asteroid leaves its orbit and it is modelled by the Sun-Earth-Moon restricted four-body problem until the asteroid is captured onto the Earth-Moon L_2 stable manifold. When the asteroid inserts onto the invariant manifold, the asteroid's motion is modelled by the Earth-Moon CRTBP problem. We have defined the patching of these two systems such that they match at the Moon-Sun three-body sphere of influence (3BSOI). Using an analytical approximation, the 3BSOI is a sphere centered at the Moon with a radius given by

$$R_{SOI} = a(\mu_{Moon} / \mu_{Sun})^{2/5} \approx 159200 km \tag{16}$$

where a is the distance between the Sun and the Earth, equal to 1AU. That is, once the asteroid is inserted into the target point on the stable manifold inside the 3BSOI of radius R_{SOI}, the asteroid is regarded to be asymptotically captured into a bound orbit around the Earth-Moon L_2 point. Therefore, as shown in Fig. 8, the target points on the stable manifolds should be chosen such that

$$\sqrt{(x-1+\mu)^2 + y^2 + z^2} \le R_{SOI} \tag{17}$$

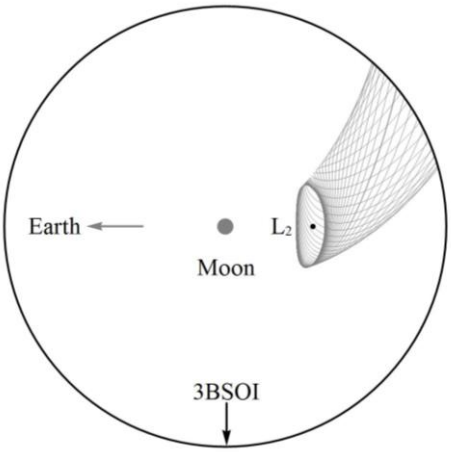

Fig. 8 Earth-Moon L_2 stable manifolds inside the 3BSOI

According to the definition of the Moon-Sun 3BSOI, we can determine the search domain of the stable manifold transfer time t_{sm}. Given one stable manifold which is determined by J and t_p, we define $t_{3BSOI}(J,t_p)$ as the stable manifold transfer time t_{sm} when the stable manifold intersects the 3BSOI for a first time. Therefore, for the stable manifolds associated with a periodic orbit with Jacobi constant J, the required set of t_{3BSOI} can be written as

$$\Gamma(J)=\bigcup_{t_p\in[0,T_p]}\left\{t_{3BSOI}(J,t_p)\right\} \tag{18}$$

and we define the maximum value of the set $\Gamma(J)$ as

$$t_{threshold}(J)=\max_{t_p\in[0,T_p]}\{\Gamma(J)\} \tag{19}$$

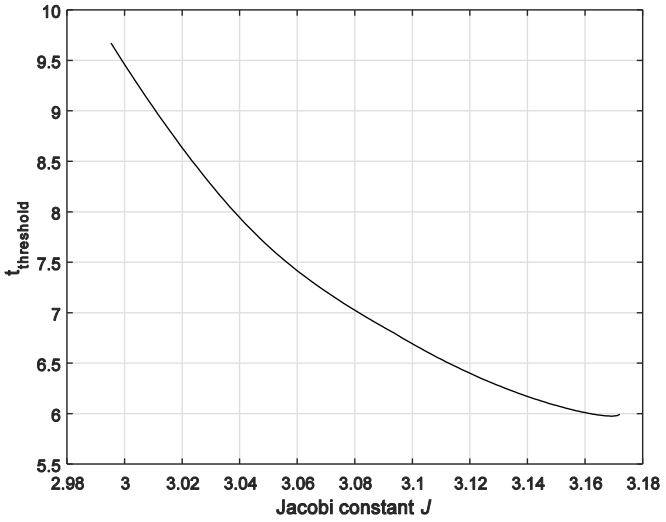

(a)

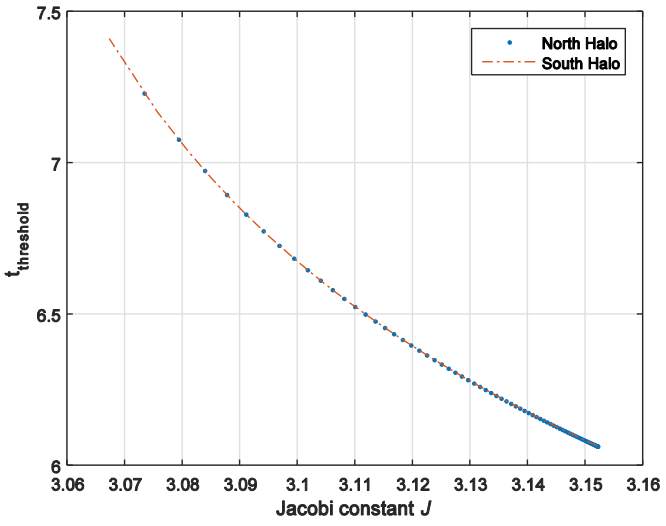

(b)

Fig. 9 $t_{threshold}$ with different Jacobi constants J (a) stable manifold associated with EM L_2 Lyapunov orbits; (a) stable manifold associated with EM L_2 Halo orbits

Therefore, $t_{threshold}(J)$ is the maximum stable manifold transfer time of the stable manifolds associated with the periodic orbit with Jacobi constant J. Therefore, it can be utilized to determine the search domain of the stable manifold transfer time t_{sm}. Figure 9 shows $t_{threshold}$ with different Jacobi constants J. In general, $t_{threshold}$ decreases when the Jacobi constant J increases and small values of J lead to large $t_{threshold}$. Since the Jacobi constant J is unknown, we have to select a limited range of the stable manifold flight time t_{sm} to fit the stable manifolds of all periodic orbits. Therefore, it is found that t_{sm} should be selected in the range [0, 9.7] for Lyapunov orbits, or [0, 7.4] for Halo orbits.

4.4 Candidate asteroid selection

To obtain appropriate candidate asteroids, the JPL Small-Body Database will be used, which represents the current catalogue of Near-Earth Objects (NEOs). It is necessary to immediately exclude NEAs with a semi-major axis or inclination much larger than the Earth's.

With the target point filter, the target point on the stable manifold which is determined by the parameters J, t_p and t_{sm} can be written as

$$P_t(J,t_p,t_{sm}) = \left\{ (x,y,z,\dot{x},\dot{y},\dot{z}) \in W^s \mid \sqrt{(x-1+\mu)^2+y^2+z^2} \le R_{SOI} \right\} \qquad (20)$$

Then the set of the target points on the stable manifolds can be obtained when we vary J, t_p and t_{sm}. Let **K** be the set of the target points which can be written as

$$\mathbf{K} = \left\{ P_t(J, t_p, t_{sm}) \mid J_{\min} \le J \le J_{\max}, 0 \le t_p \le T_p, 0 \le t_{sm} \le t_{threshold} \right\} \tag{21}$$

where $J_{\min} = 2.99533289$, $J_{\max} = 3.17205221$ and $t_{threshold} = 9.7$ for the planar Lyapunov orbits while $J_{\min} = 3.06733209$, $J_{\max} = 3.15211497$ and $t_{threshold} = 7.4$ for the halo orbits.

Now that the set of target points is known, it is possible to calculate the three-dimensional orbital element space (the semi-major axis, eccentricity and inclination (a, e, i)) of the candidate NEAs which can be captured onto Earth-Moon L_2 periodic orbits under a certain Δv threshold. The design procedure is presented as follows,

(1) Given one approach date T_f, transform the set of target points **K** to the Sun-centered inertial frame by using Eq. (7) and Eq. (8) and then obtain the three-dimensional orbital element space of the target points in the Sun-centered inertial frame, shown in Fig. 10;

(2) Add an impulse $\Delta \boldsymbol{v}_2 = \|\Delta \boldsymbol{v}_2\| \bullet [\cos p_2 \cos q_2, \cos p_2 \sin q_2, \sin p_2]$ $\left(\|\Delta \boldsymbol{v}_2\| \le \Delta v, p_2 \in [0, \pi], q_2 \in [0, 2\pi] \right)$ at these target points on the EM L_2 stable manifolds and propagate these states backwards (with propagation time T (days)) in the Sun-Earth-Moon restricted four-problem model and then obtain the final states;

(3) Add another impulse $\Delta \boldsymbol{v}_1 = \|\Delta \boldsymbol{v}_1\| \bullet [\cos p_1 \cos q_1, \cos p_1 \sin q_1, \sin p_1]$ $\left(\|\Delta \boldsymbol{v}_1\| \le \Delta v - \|\Delta \boldsymbol{v}_2\|, p_1 \in [0, \pi], q_1 \in [0, 2\pi] \right)$ at these final states and then calculate the three-dimensional orbital element space (a, e, i) of these states after $\Delta \boldsymbol{v}_1$ is added;

(4) Vary the approach date T_f, propagation time T ($T \in [0, 1000\, days]$), two impulses $\Delta \boldsymbol{v}_1$ and $\Delta \boldsymbol{v}_2$ and obtain the three-dimensional orbital element space (a, e, i) of the candidate NEAs that can potentially be captured under the Δv threshold.

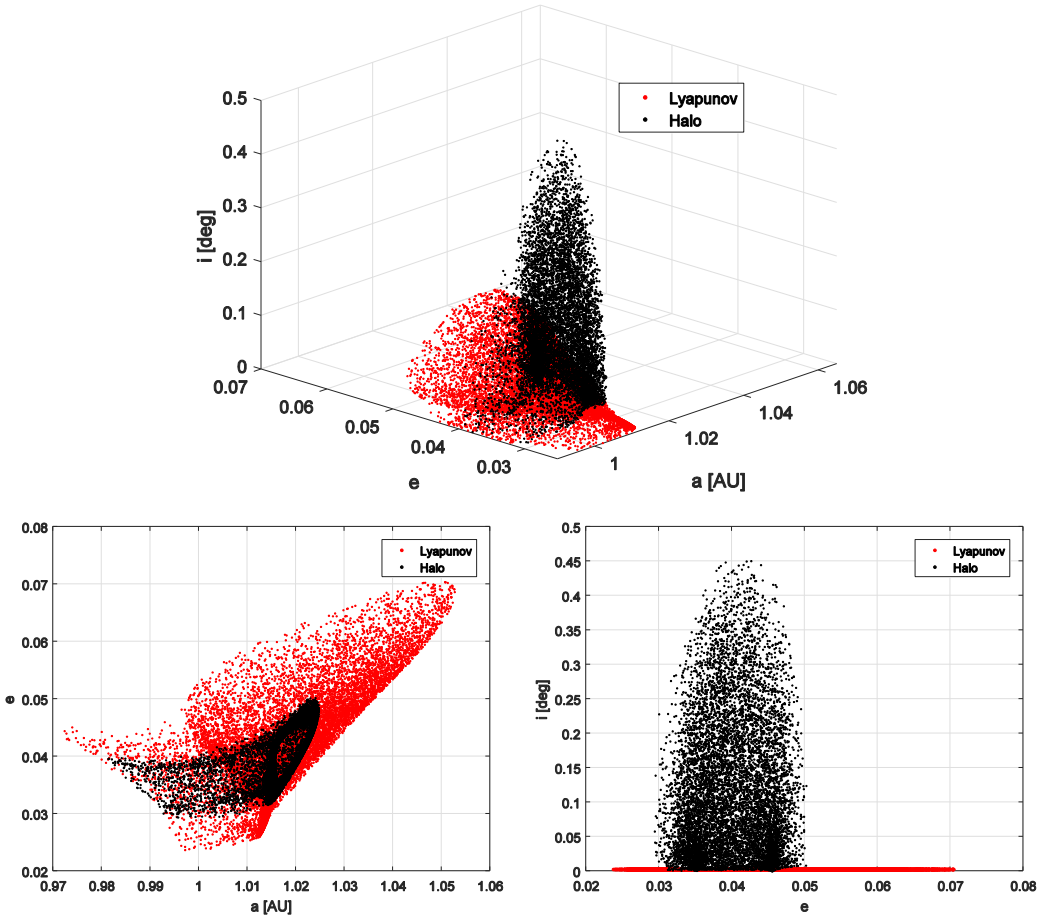

Fig. 10 Given T_f=63000 [MJD], the three-dimensional orbital element space of target points on the stable manifolds associated with EM L_2 Lyapunov orbits (red) and Halo orbits (black).

According to the design procedure above, the three-dimensional orbital element space of candidate NEAs is plotted in Fig. 11 and Fig. 12 for transfers to the EM L_2 stable manifolds with a Δv threshold of 500 ms^{-1}, as used by Yárnoz et al (2013). With a free phase, any asteroid with orbital elements inside these regions can be captured with a total Δv cost below 500 ms^{-1}. With this filter, the candidate asteroids are listed in Table 1.

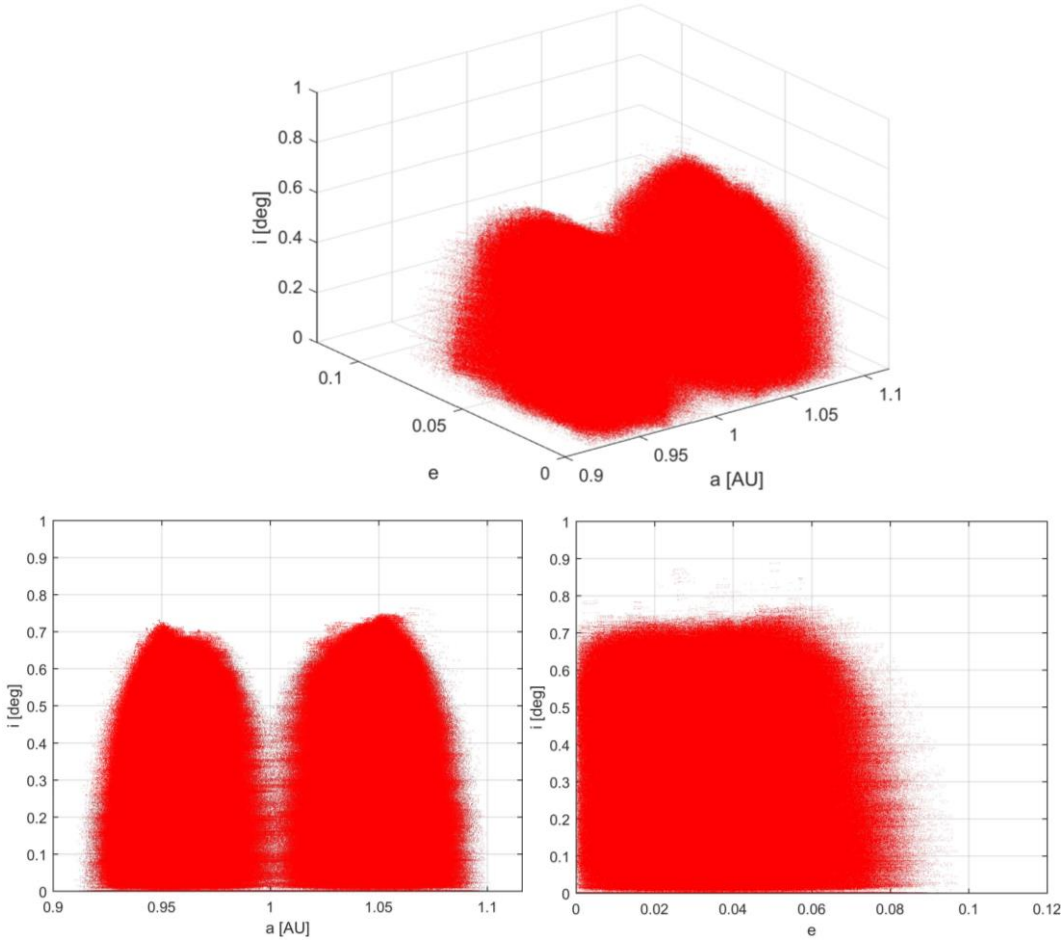

Fig. 11 Three-dimensional orbital element space of the stable manifold associated with EM L_2 Lyapunov orbits with a Δv threshold of 500 ms^{-1}

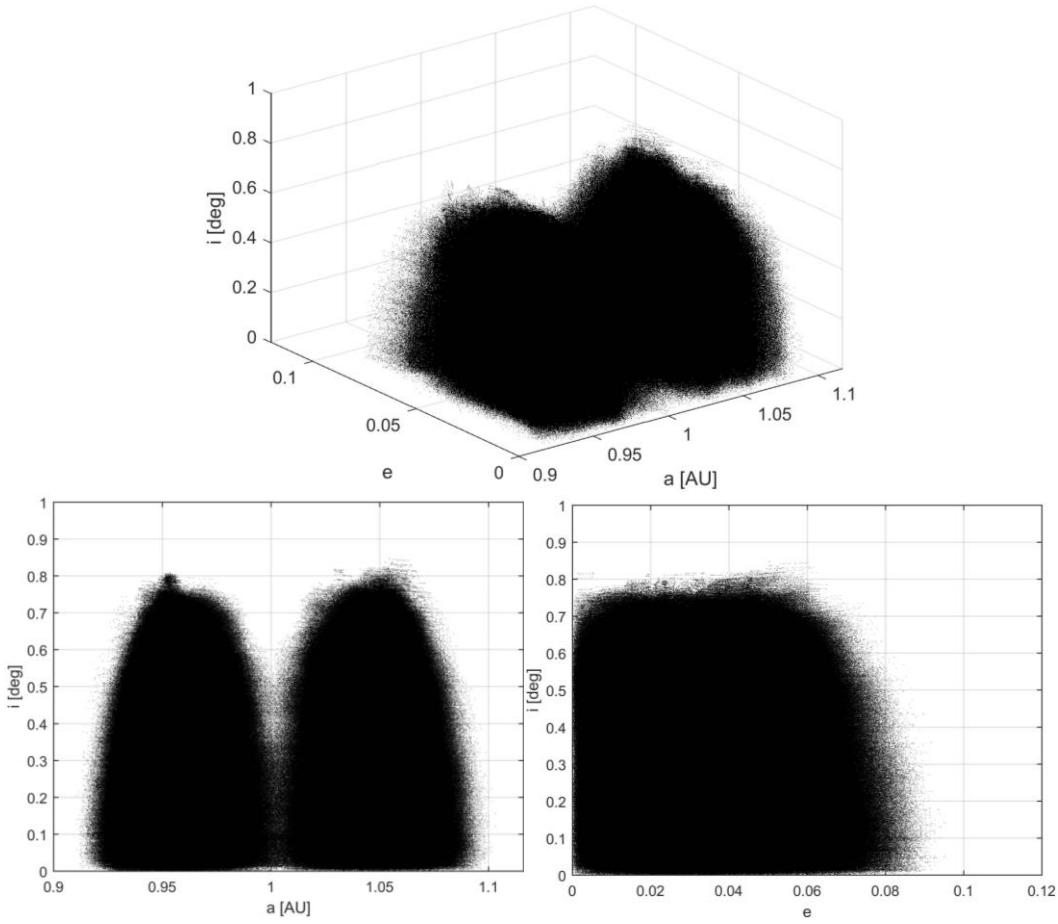

Fig. 12 Three-dimensional orbital element space of the stable manifold associated with EM L_2 Halo orbits with a Δv threshold of 500 ms^{-1}

Table 1 Orbital elements of the candidate near-Earth asteroids

NEA	*a* [AU]	*e*	*i* [deg]
2000SG344	0.977522	0.066887	0.111360
2006RH120	1.033272	0.024486	0.595310
2007UN12	1.053745	0.060483	0.235350
2008EA9	1.059120	0.079778	0.424640
2008UA202	1.033231	0.068587	0.263870
2009BD	1.008614	0.040818	0.385160
2010UE51	1.055203	0.059705	0.624280
2014WX202	1.035161	0.058858	0.412600
2014QN266	1.052702	0.092276	0.487980
2015PS228	1.037622	0.079409	0.791510

4.5 Approach date and departure date guess

For a candidate asteroid, there exists a date when the asteroid has its closest approach to the Earth. Here we define this date as the moment of minimum distance (MOMD) between the asteroid and the Earth. The distance between the candidate asteroid and the Earth can be calculated by propagating the candidate asteroid's initial state forward in the Sun-Earth-Moon restricted four-body problem and then the MOMD can be obtained, an example of which is shown in Fig. 13. Since we are interested in low-cost transfers with a total Δv cost below 500 ms^{-1}, the first impulse should be smaller than this value and then the asteroid's new orbit after the first impulse can be considered to be proximal to its former orbit. Therefore, we can still estimate the date when the asteroid's closest approach to the Earth is nearby the MOMD. Therefore, the approximate range of approach date can be written as

$$[\mathrm{MOMD} - T_{period}, \mathrm{MOMD} + T_{period}] \tag{22}$$

where T_{period} is the asteroid's orbit period about the Sun.

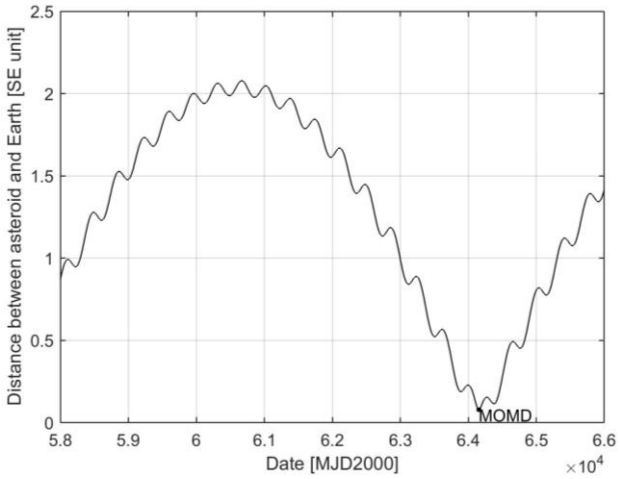

Fig. 13 Approach date guess by using MOMD (2014WX202)

The Lambert arc in the two-body problem with two impulses can now be used as an initial guess of the departure date when the first impulse is applied and the asteroid transfers towards the target point in the Earth-Moon system. There are 2 variables in this problem: the departure date T_0 and the transfer time T_{fly} (or the approach date T_f). Then, the total cost of the Lambert transfer can be calculated as

$$\delta v = \|\delta \boldsymbol{v}_1\| + \|\delta \boldsymbol{v}_2\| \tag{23}$$

where $\delta \boldsymbol{v}_1, \delta \boldsymbol{v}_2$ are the first impulse and second impulses, respectively.

Since we only consider the influence of the Sun's gravity here, the total δv cost must be different from the result in the Sun-Earth-Moon restricted four-body problem model. However, we can still use the first Lambert impulse $\delta \boldsymbol{v}_1$ to guess the first impulse $\Delta \boldsymbol{v}_1$ in Sun-Earth-Moon restricted four-body model. Since we expect to find an asteroid which can be captured directly with $\Delta v \leq 500$ ms^{-1}, here we set 500 ms^{-1} as a threshold for $\delta \boldsymbol{v}_1$ and then guess the departure date T_0. As shown in Fig.8, the target points are defined in a limited region around the Moon (3BSOI). Thus, there should be only a marginal difference between the first impulse of the Lambert to the Moon and the first impulse of the Lambert arc to the target points. Therefore, for simplification, the target position for the Lambert arc is assumed to be the center of the Moon, in order to provide a guess in the search domain of the departure date T_0, shown in Fig. 14.

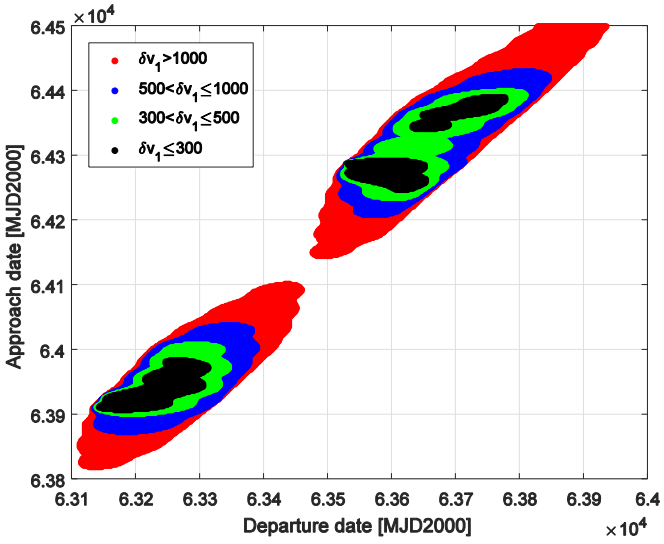

Fig. 14 The first impulse δv_1 (ms^{-1}) as a function of T_0 and T_f (2014WX202)

4.6 Design procedure

The process of calculating the transfer trajectories from the candidate asteroid's orbit to the EM L_2 stable manifold is as follows:

(1) Select one target asteroid among the list of candidate asteroids (e.g., 2014WX202) in Table 1;

(2) Guess the range of the approach date using Eq. (22);

(3) Assume that the Moon is the target position for the Lambert arc from the candidate asteroid's orbit and then guess the search domain of departure date T_0

and approach date T_f, corresponding to the first impulse $\|\delta \boldsymbol{v}_1\| \le 500\,\mathrm{ms}^{-1}$, as shown in Fig. 15;

(4) Given a Jacobi constant J, t_p and t_{sm}, the target point on the EM L_2 stable manifolds are determined and then transformed to the Sun-centered inertial frame by using Eq.(7) and Eq. (8);

(5) The Lambert arc in the Sun-centered two-body problem is utilized to design the transfer to the target points from the candidate asteroid's orbit and so the first impulse can be estimated;

(6) Based on the initial guess of the first impulse, the differential correction in Eq. (15) is utilized to design the transfer trajectory to the target point from the candidate asteroid's orbit;

Then we can obtain the capture trajectory for a candidate asteroid to the Earth-Moon L_2 periodic orbit, as shown in Fig. 15.

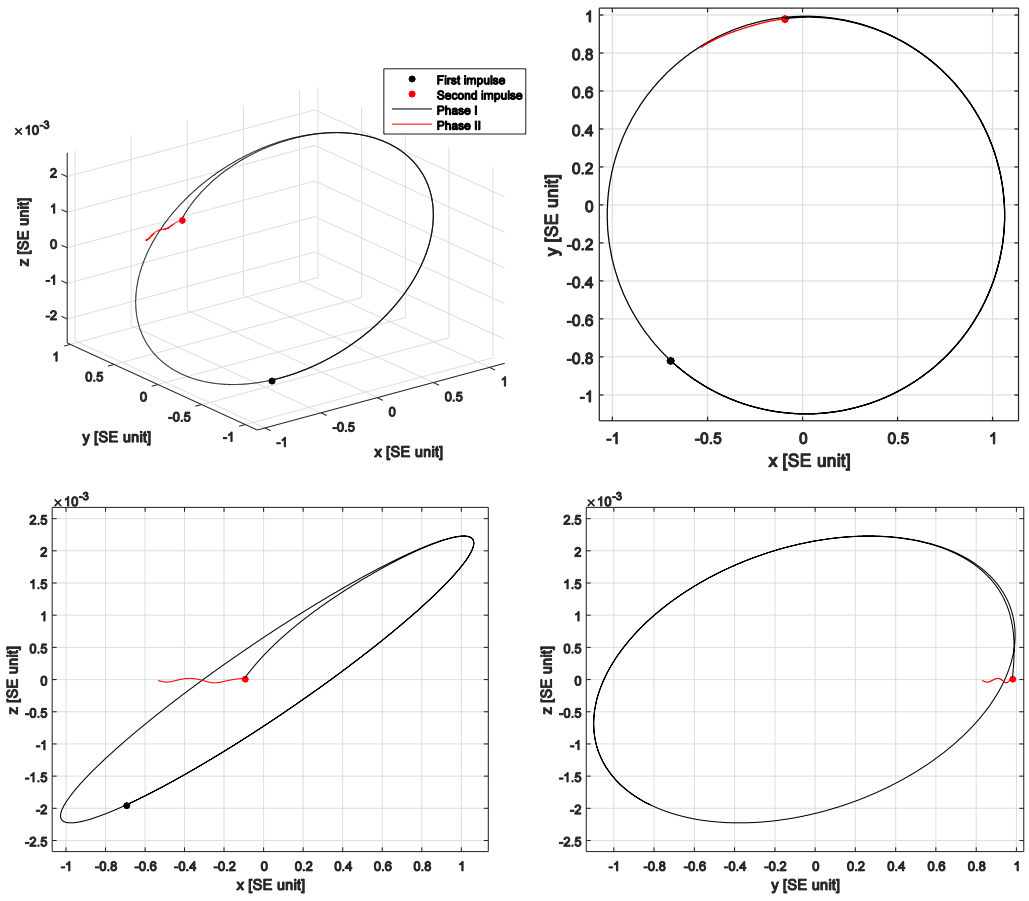

Fig. 15 Given T_0 = 63310 [MJD], T_f= 63954[MJD], J = 3.14658338, t_p = 0.66, t_{sm} = 5.0, direct capture trajectory (phase I) for 2014WX202 to an Earth-Moon L_2 north halo orbit and stable manifold (phase II) associated with the target halo orbit in the J2000 Sun-cantered inertial frame

4.7 Optimization and discussion

For each candidate NEA, feasible approach dates are assumed in the interval 2016–2050. The orbital elements of the candidate asteroids are assumed to be valid until their next close approach to the Earth. Thus, for each candidate asteroid, there are 5 variables: (T_0, T_f, J, t_p, t_{sm}). These transfer trajectories between the candidate asteroid initial orbits and the stable manifolds can be searched using NSGA-II, a global optimization method which is based on a multi-objective evolutionary algorithm (Deb et al. 2002), using the total Δv cost as the objective function. Then transfers obtained with NSGA-II can be locally optimized with sequential quadratic programming (SQP), implemented in the function *fmincon* in MATLAB. Therefore, we find that 6 NEAs that can be captured with a total Δv cost of less than 500 ms^{-1}, shown in Table 2. It can be seen that the optimal departure date for a given NEA is almost the same for different target periodic orbits around the Earth-Moon L_2 point (i.e., Halo orbits and Lyapunov orbits), as well as the approach date.

Comparing the direct capture strategy to Earth-Moon libration point orbits (LPOs) and the capture strategy into Sun-Earth LPOs in prior studies (Yárnoz et al. 2013; Sánchez and Yárnoz 2016), we note that the one of the obvious differences between these two capture strategies is the flight time along the stable manifolds. That is, the direct capture of the asteroids into the Earth-Moon (LPOs) needs a much shorter flight time along the stable manifolds associated with Earth-Moon LPOs, while the capture onto Sun-Earth LPOs requires a longer time for the asteroid to be asymptotically captured through utilizing the stable manifolds associated with the Sun-Earth LPOs.

Without utilizing the Earth-Moon L_2 stable manifolds, the transfer trajectory of the direct capture of the NEAs to the Earth-Moon L_2 target periodic orbit is also modeled in the Sun-Earth-Moon restricted four-body problem. The Lambert arc in the Sun-asteroid two-body problem is used as an initial guess and then the differential correction is used to calculate the transfer trajectory from the asteroid's initial obit to Earth-Moon L_2 target periodic orbit. The optimal results of the direct capture of the NEAs to the Earth-Moon L_2 target periodic orbit without utilizing the Earth-Moon L_2 stable manifolds are shown in Table 3. Comparing the results in Table 2 and Table 3, it can be seen that direct capture using the stable manifolds is cheaper than direct capture without utilizing the

stable manifolds. It can be concluded that the Earth-Moon L_2 stable manifolds can provide greater opportunities to achieve cheaper NEA capture.

Table 2 Results of optimal direct capture of asteroid to EM L_2 periodic orbits using the stable manifolds

NEA	Δv_1 (ms^{-1})	Δv_2 (ms^{-1})	Δv (ms^{-1})	T_0 [MJD]	T_{fly} (day)	J	Target (Earth-Moon)
2014WX202	244.06	92.88	336.94	63329.7	668.8	3.15122014	L_2 Halo
	254.64	66.31	320.95	63334.0	664.3	3.07131868	L_2 Lyapunov
2000SG344	327.73	40.56	368.29	61756.1	247.3	3.10676604	L_2 Halo
	311.22	134.10	445.32	61764.4	236.9	3.14377539	L2 Lyapunov
2010UE51	268.85	133.82	402.67	59444.0	851.4	3.12105929	L_2 Halo
	336.40	64.14	400.54	59453.3	844.3	3.08113259	L_2 Lyapunov
2008EA9	199.81	208.52	408.34	58694.2	172.4	3.14914863	L_2 Halo
	265.04	165.75	430.80	58678.0	193.4	3.07462228	L_2 Lyapunov
2007UN12	202.62	335.68	538.30	58838.2	292.0	3.10872264	L_2 Halo
	334.17	149.11	483.28	58933.5	177.1	3.07297449	L_2 Lyapunov
2006RH120	331.33	123.30	454.63	61089.8	1011.8	3.10603901	L_2 Halo
	353.30	126.70	480.00	61084.0	1013.6	3.12138131	L_2 Lyapunov

Table 3 Results of optimal direct capture of asteroid to EM L_2 periodic orbits without using the stable manifolds

NEA	Δv_1 (ms^{-1})	Δv_2 (ms^{-1})	Δv (ms^{-1})	T_0 [MJD]	T_{fly} (day)	J	Target (Earth-Moon)
2014WX202	249.23	251.34	500.57	63331.0	643.9	3.14495182	L_2 Halo
	242.91	225.12	468.03	63338.7	636.8	3.13679076	L_2 Lyapunov
2000SG344	316.65	133.08	449.73	61772.6	206.3	3.06733209	L_2 Halo
	266.22	269.25	535.47	61741.6	206.7	3.03647927	L_2 Lyapunov
2010UE51	310.82	227.45	538.27	59446.0	848.0	3.10393415	L_2 Halo
	335.90	159.09	494.99	59453.2	841.2	3.07626202	L_2 Lyapunov
2008EA9	218.93	244.42	463.35	58688.0	155.9	3.14546217	L_2 Halo
	202.56	270.07	472.63	58686.4	157.6	3.12539870	L_2 Lyapunov
2007UN12	208.57	344.25	552.82	58831.0	274.6	3.06733209	L_2 Halo
	183.20	449.90	633.10	58843.5	262.1	3.09682549	L_2 Lyapunov
2006RH120	350.62	203.72	554.34	61079.5	994.5	3.12951683	L_2 Halo
	352.26	246.33	598.59	61080.2	966.7	3.15866013	L_2 Lyapunov

5 Indirect capture of near-Earth asteroids to Earth-Moon L_2 periodic orbits

Another type of lunar capture of NEAs will be termed indirect capture. In this capture strategy, the asteroid capture trajectories are designed in a patched three-body model which consists of the Sun-Earth (SE) and Earth-Moon (EM) systems (Mingotti et al. 2014b), based on the work of Sanchez and McInnes (2011), Sanchez et al. (2012) and Yárnoz et al. (2013). As an approximation of the Sun-Earth-Moon four-body problem, the patched three-body model can be decomposed into the Sun-Earth CRTBP system and the Earth-Moon CRTBP system. It is assumed that the Earth–Moon CRTBP system is coplanar with the Sun–Earth CRTBP system. Thus, asteroid capture trajectories can be accomplished by patching together the unstable manifolds in the Sun-Earth CRTBP system and the stable manifolds in the Earth-Moon CRTBP system. It should be noted that the patching points of the two invariant manifolds are defined by the chosen Poincaré section (angle γ), shown in Fig. 16. The design procedure

for the indirect capture of NEAs by using these patched three-body problems can be divided into three parts as follows;

(1) With the initial impulse $\Delta \boldsymbol{v}_1$, the asteroid leaves its orbit and is injected onto the stable manifolds associated with the Sun-Earth L_1/L_2 points with the second impulse $\Delta \boldsymbol{v}_2$. These two impulsive burns can be solved by using the Lambert arc in the two-body problem (Yárnoz et al. 2013);

(2) After the NEA inserts onto the stable manifolds, it will be asymptotically captured onto a periodic orbit around the Sun-Earth L_1/L_2 point; the asteroid will be on the periodic orbit until it reaches the point where the Sun-Earth unstable manifold is propagated forward from; then the asteroid leaves the periodic orbit by utilizing the unstable manifold and then approaches the injection plane between the Sun-Earth unstable manifold and the Earth-Moon L_2 stable manifolds;

(3) With the third impulse $\Delta \boldsymbol{v}_3$, the NEA inserts onto the Earth-Moon L_2 stable manifold and will be asymptotically captured onto a periodic orbit around the Earth-Moon L_2 point.

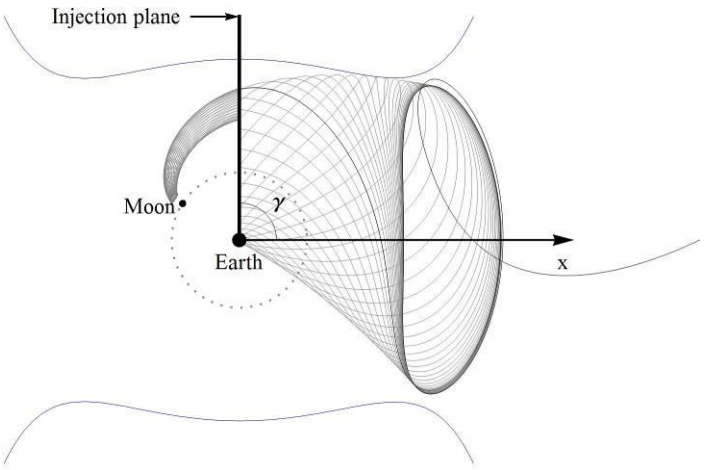

Fig. 16 Indirect asteroid capture in the patched three-body problem with the Poincaré section shown

In this problem, there are 9 variables as follows:

- T_0: departure date when the first impulse $\Delta \boldsymbol{v}_1$ is applied to the candidate asteroid and the asteroid leaves its orbit;

- T_f: approach date corresponding to the date when the candidate asteroid inserts into the SE (Sun-Earth) L_1/L_2 stable manifolds with the second impulse $\Delta \boldsymbol{v}_2$;
- t_{sm}: SE L_1/L_2 stable manifold transfer time;
- J_{SE}: Jacobi constant of target periodic orbit around SE L_1/L_2;
- t_{p1}: time determining the point on the target periodic orbit around SE L_1/L_2 where the SE L_1/L_2 stable manifold is propagated backward from;
- t_{p2}: time determining the point on the target periodic orbit around SE L_1/L_2 where the SE L_1/L_2 unstable manifolds is propagated forward from;
- γ: angle determining the injection plane where the SE L_1/L_2 unstable manifold and EM L_2 stable manifold are patched together with the third impulse $\Delta \boldsymbol{v}_3$;
- J_{EM}: Jacobi constant of EM target periodic orbit;
- t_{p3}: time determining the point on the target periodic orbit around EM L_2 where the EM L_2 stable manifold is propagated backward from.

These 9 variables can be divided into two parts: (T_0, T_f, $\boldsymbol{t_{sm}}$, J_{SE}, t_{p1}) and (J_{SE}, t_{p2}, γ, J_{EM}, t_{p3}), corresponding to those associated with capturing the asteroid onto the Sun-Earth stable manifold (Part I) and those associated with patching together the Sun-Earth unstable manifold and Earth-Moon L_2 stable manifold (Part II), respectively. However, there exists a time constraint between the two parts. That is, once the variables (T_0, T_f, $\boldsymbol{t_{sm}}$, J_{SE}, t_{p1}, t_{p2}, γ) are given, the Sun-Earth unstable manifold is propagated forward until it reaches the Poincaré section (angle γ) and then the Sun-Earth unstable transfer time t_{um} is determined; accordingly, the position of the Moon is determined.

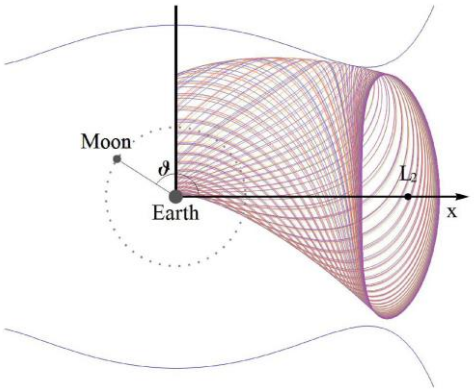

(a)

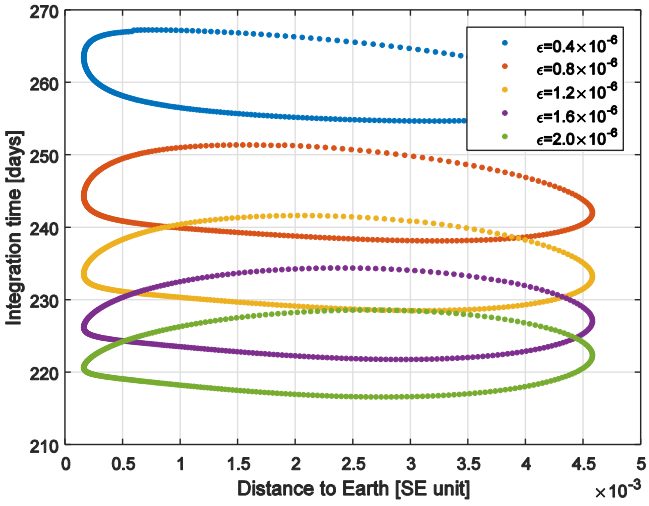

(b)

Fig. 17 (a) Unstable manifolds of Sun-Earth L_2 Lyapunov orbit (J=3.0008289345) and (b) their integration time to the same Poincaré section (x = 1-μ_{se}) with varying $\varepsilon \in [0.4\times10^{-6}, 2\times10^{-6}]$

It should be noted that small values of ε in Eq. (5) can result in large integration times when calculating the unstable manifolds. Figure 17(b) shows that the integration time of the Sun-Earth unstable manifolds to the same Poincaré section clearly changes when we vary the value of ε. This means even given the values of (t_0, t_f, t_{sm}, J_{SE}, t_{p1}, t_{p2}, γ), the position of the Moon can be anywhere along its orbit, as long as an appropriate value of ε is selected. Therefore, we can introduce a variable ϑ ($0 \le \vartheta < 2\pi$) determining the position of the Moon, shown in Fig. 17(a) and the variables of Part II are extended to (J_{SE}, t_{p2}, γ, J_{EM}, t_{p3}, ϑ). The common parameter between the two parts is the Jacobi constant J_{SE} of the target periodic orbit in the Sun-Earth system. Part II can then be optimized by using NSGA-II. During each step in optimizing Part II, there is a specific value of J_{SE} and given this value, Part I can be optimized by using the function *fmincon* in MATLAB. Therefore, this problem can be optimized with total Δv cost as the

objective function. The results of the indirect capture of the NEAs are listed in Table 4 and the optimal capture trajectory for 2014WX202 to an Earth-Moon L_2 Lyapunov orbit is shown in Fig. 19. It should be noted that the in the Table 4 and Table 5, 2L, 2H, 1L, 1H are short for the planar Lyapunov orbit around L_2, the Halo orbit around L_2, the planar Lyapunov orbit around L_1 and the Halo orbit around L_1, respectively.

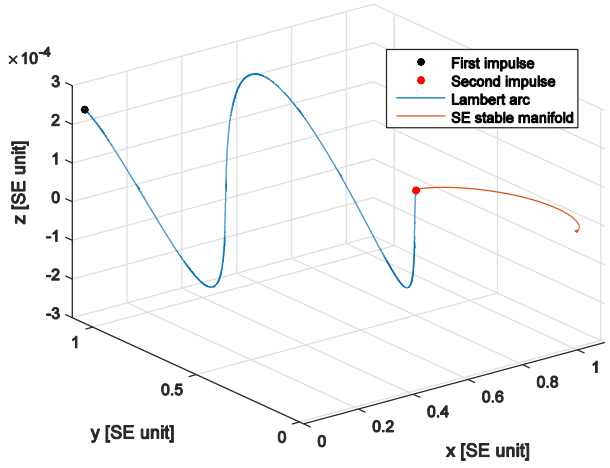

(a)

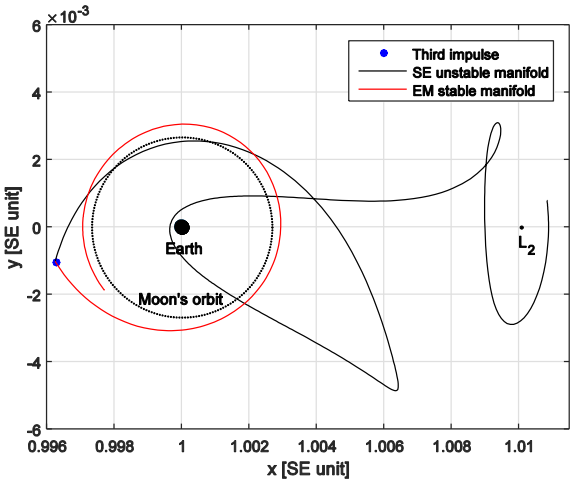

(b)

Fig. 18 Indirect capture trajectory for 2014WX202 to Earth-Moon L_2 Lyapunov orbit in the Sun-Earth rotating frame: (a) the transfer trajectory of Part I (b) the transfer trajectory of Part II

Table 4 Results of optimal indirect capture of asteroids to Earth-Moon L_2 periodic orbits

NEA	$\Delta v_1+\Delta v_2$ (ms^{-1})	Δv_3 (ms^{-1})	Δv (ms^{-1})	T_0 [MJD]	T_{fly} (day)	J_{EM}	J_{SE}	Target (SE+ EM)
	393.21	14.43	407.64	62558.3	1337.5	3.11018496	3.00051125	2L+2L
2014	397.51	52.14	449.65	63027.3	1392.5	3.14985969	3.00025026	2L+2H
WX202	403.85	80.94	484.79	61934.3	1886.1	3.11586792	3.00082448	2H+2L
	367.31	154.46	521.77	61909.2	2140.1	3.0889044	3.00079312	2H+2H
	455.90	15.80	471.70	60415.7	1277.9	3.12138131	3.00037998	1L+2L
2000	479.89	59.080	538.97	60421.2	1410.6	3.15211412	3.00078111	1L+2H
SG344	487.19	63.23	550.42	60418.6	1149.4	3.00079852	3.00079852	1H+2L
	467.74	138.85	606.59	60407.0	1246.1	3.15211412	3.00078086	1H+2H
	387.57	8.58	396.15	58456.9	1937.8	3.07462228	3.00043118	2L+2L
2010	377.52	82.550	460.07	58452.5	2052.3	3.15211412	3.00043478	2L+2H
UE51	514.13	1.06	515.19	58064.6	1653.3	3.13310905	3.00082488	2H+2L
	482.01	84.230	566.24	58065.5	1892.4	3.13478422	3.00081888	2H+2H
	436.70	8.12	444.82	57945.9	1272.6	3.02908121	3.00023845	2L+2L
2008	436.86	126.40	563.26	57947.9	1298.9	3.15211412	3.00023845	2L+2H
EA9	719.92	76.570	796.49	57882.9	1624.2	3.10285713	3.00082452	2H+2L
	703.51	36.670	740.18	57864.5	1435.7	3.14031595	3.00082333	2H+2H
	333.80	12.81	346.61	58248.2	1291.7	3.07297450	3.00066499	2L+2L
2007	333.80	73.720	407.52	58247	1156.6	3.15211412	3.00066499	2L+2H
UN12	446.31	40.88	487.19	58101.8	1197.4	3.13185538	3.00082448	2H +2L
	397.66	84.230	481.89	58241.2	1320.7	3.13478422	3.00081888	2H+2H
	317.39	11.49	328.88	59649.2	2295.3	3.16778325	3.00066086	2L+2L
2006	320.24	69.210	389.45	59653.4	2370.6	3.15211412	3.00067012	2L+2H
RH120	308.62	66.75	375.37	60465.6	1488.4	3.13310905	3.00082333	2H+2L
	308.62	36.670	345.29	60465.6	1727.1	3.14031595	3.00082333	2H+2H

Table 5 Results of optimal indirect capture of asteroids to Earth-Moon L_2 periodic orbits without using the Earth-Moon stable manifolds

NEA	$\Delta v_1+\Delta v_2$ (ms^{-1})	Δv_3 (ms^{-1})	Δv (ms^{-1})	T_0 [MJD]	T_{fly} (day)	J_{EM}	J_{SE}	Target (SE+ EM)
	393.21	43.84	437.05	62558.3	1575.4	3.10581721	3.00051125	2L +2 L
2014	397.51	66.40	463.91	63027.3	1581.7	3.14985969	3.00025026	2L + 2H
WX202	403.85	74.87	478.72	61934.3	2271.2	3.12138131	3.00082448	2H + 2L
	492.41	112.74	605.15	61549.1	2605.3	3.14406769	3.0008234	2H+ 2H
	455.90	25.41	481.31	60415.7	1859.3	2.99745601	3.00037998	1L +2 L
2000	489.33	99.89	589.22	60408	1618.1	3.15211412	3.00078111	1L + 2H
SG344	490.85	55.64	546.49	59331.6	1595	3.14150569	3.00083043	1H + 2L
	497.19	165.61	662.80	59322.8	1594.4	3.15200176	3.00083042	1H+ 2H
	366.55	36.84	403.39	58456.9	2019	3.16337677	3.00043118	2L +2 L
2010	379.99	89.69	469.68	58450.6	2025.9	3.15211412	3.00043478	2L + 2H
UE51	487.30	105.05	592.35	58065.6	2049.9	3.11864645	3.0008234	2H + 2L
	482.01	199.79	681.80	58065.5	1731.3	3.1521004	3.00081888	2H+ 2H
	436.70	70.30	507.00	57945.9	1526.4	3.09682549	3.00023845	2L +2 L
2008	438.11	217.69	655.80	57946.2	1272.6	3.14985969	3.00023857	2L + 2H
EA9	719.92	72.71	792.63	57882.9	1526.6	3.12138131	3.00082452	2H + 2L
	719.92	36.63	756.55	57882.9	1359.4	3.15195881	3.00082452	2H+ 2H
	333.80	52.33	386.13	58247	1294.6	3.16926055	3.00066499	2L +2 L
2007	312.59	80.33	392.92	58603.2	1014.0	3.15211412	3.00066499	2L + 2H
UN12	411.50	72.71	484.21	58241.6	1419.9	3.12138131	3.00082452	2H + 2L
	464.13	75.15	539.28	58108.4	1398.3	3.13860082	3.00081873	2H+ 2H
	317.39	16.85	334.24	59649.2	2514.7	3.17193855	3.00066086	2L +2 L
2006	319.76	89.32	409.08	59653.4	2557.7	3.15211412	3.00067012	2L + 2H
RH120	328.35	74.87	403.22	60699.2	1578.5	3.12138131	3.00082448	2H + 2L
	308.62	158.44	467.06	60465.6	1774.3	3.15184498	3.00082333	2H+ 2H

Comparing the results in the Table 2 and Table 4, we find that the direct capture to the Earth-Moon L_2 point needs a shorter flight time and so chemical propulsion may be preferred for this capture strategy. On the other hand, the indirect asteroid capture always needs a much longer flight time. Therefore, low-thrust propulsion can be more easily applied to the indirect capture strategy. For comparison, the optimal results of the indirect capture of NEAs to the Earth-Moon L_2 target periodic orbit without utilizing the Earth-Moon L_2 stable manifolds are shown in Table 5. It is assumed that the transfer trajectories for indirect asteroid capture can be designed by patching the Sun-Earth unstable manifolds and the Earth-Moon L_2 periodic orbits directly. Comparing the results in Table 4 and

Table 5, we can find that the indirect capture strategy using the Earth-Moon stable manifolds can easily achieve cheaper captures.

From Table 4 and Table 5, we find that it is cheapest to patch together the Sun-Earth Lyapunov unstable manifold and Earth-Moon Lyapunov stable manifold than to patch other combinations of the Sun-Earth unstable manifolds and Earth-Moon stable manifolds, e.g. the Sun-Earth Halo unstable manifold and Earth-Moon Halo stable manifold. This is because in the patched three-body problem it is assumed that the motion of all four bodies are in the same plane. Patching the Sun-Earth Lyapunov unstable manifold and Earth-Moon Lyapunov stable manifold together is a planar problem and we do not need to consider the *z*-component of the manifolds. Therefore, we have more opportunities to patch the Sun-Earth Lyapunov unstable manifold and Earth-Moon Lyapunov stable manifold together, while there are only two intersection points between one Sun-Earth Halo unstable manifold and one Earth-Moon Halo stable manifold, as well as one Sun-Earth Halo unstable manifold and one Earth-Moon Lyapunov stable manifold, one Sun-Earth Lyapunov unstable manifold and one Earth-Moon Halo stable manifold, shown in Fig. 19.

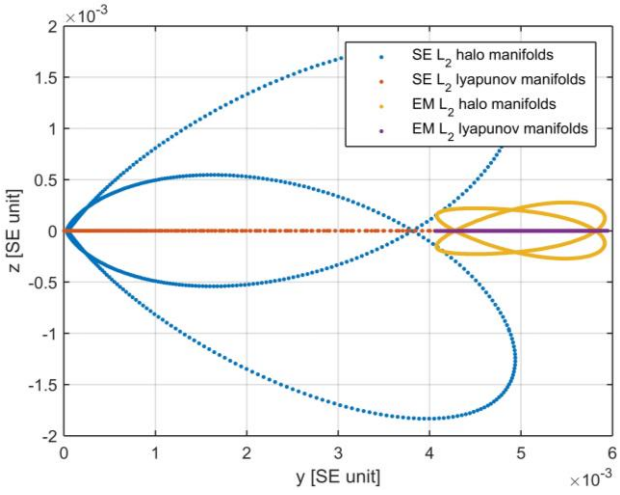

Fig. 19 Projection of SE L_2 manifolds (J=3.000738) and EM L_2 manifolds (J=3.00095, $\mathscr{O}$=0.5π) on Poincar ésection (x = 1-μ_{se}) in the Sun-Earth rotating frame

6 Direct and indirect capture of near-Earth asteroids to triangular points in the Earth-Moon system

In the ideal CRTBP model, the triangular points L_4/L_5 are stable. Even when we take the eccentricity of the lunar orbit and the influence of the solar radiation pressure into account, the instability of the triangular points is still much milder than that of the collinear points (Zhang and Hou 2015). This means that station-keeping does not require significant energy. Therefore, the vicinity of the triangular points in Earth-Moon system could be a preferred location for captured NEAs. However, the stability properties of the triangular points are also a disadvantage because there are no dynamical structures such as the stable or unstable invariant manifolds associated with the triangular points which can be utilized to design low-cost transfer trajectories.

The linearized solution in the x–y plane around triangular points can be expressed as (Szebehely 1967; Zhang and Hou 2015):

$$\begin{cases} \xi = C_1 \cos\theta_1 + C_2 \cos\theta_2 \\ \eta = m_1 C_1 \cos\theta_1 + n_1 C_1 \sin\theta_1 + m_2 C_2 \cos\theta_2 + n_2 C_2 \sin\theta_2 \end{cases} \tag{24}$$

where

$$m_i = -\Gamma_i \Omega_{xy}^0 , n_i = -2\omega_i \Gamma_i , \Gamma_i = \frac{1}{\omega_i^2 + \Omega_{yy}^0} \quad \theta_i = \omega_i t + \varphi_i \ (i=1, 2)$$

$$\Omega_{xy} = \frac{\partial}{\partial y}\left(\frac{\partial \Omega}{\partial x}\right), \Omega_{yy} = \frac{\partial^2 \Omega}{\partial y^2}, \omega_1 \cong \frac{27}{4}\mu, \omega_2 \cong 1 - \frac{27}{8}\mu , \Omega_{yy} = \frac{\partial^2 \Omega}{\partial y^2}, \quad , \omega_2 \cong 1 - \frac{27}{8}\mu$$

and $\Omega_{xy}^0 , \Omega_{yy}^0$ are the values of $\Omega_{xy} , \Omega_{yy}$ at the triangular points, respectively.

There are two kinds of periodic orbits around the triangular points, long-period orbits and short-period orbits which are defined by the components ω_1 and ω_2, respectively (Szebehely 1967). The coefficients C_1, C_2 correspond to the amplitudes of the short periodic orbit and long periodic orbit, respectively. In addition $\varphi_i \ (i = 1, 2)$ represents the initial phase angle. Generally speaking, the short-period orbits are much more stable than the long-period orbits, under given perturbations. Therefore, we choose the short-period orbits as the target orbit with $C_1 = 0$ and $C_2 \leq 0.2$ (Zhang and Hou 2015) , shown in Fig. 20.

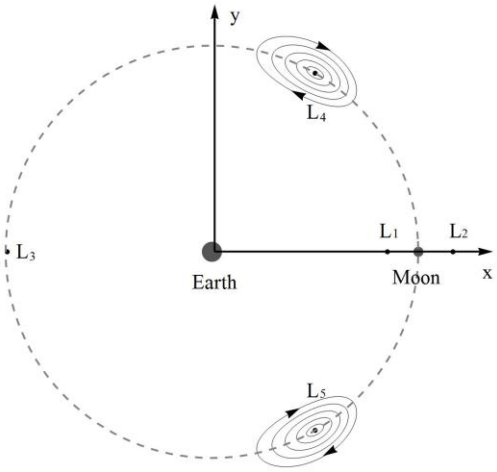

Fig. 20 Short-period orbit around the triangular points L_4/L_5 in the Earth-Moon system (C_1=0, $C_2 \leq 0.2$)

Similar to the direct/indirect asteroid capture to periodic orbits around the Earth-Moon L_2 point, there also exist two types of asteroid capture strategies and so we can still apply the design procedures of Section 3-4 to design the direct/indirect capture of asteroids to the triangular points. However, different to the transfers to the Earth-Moon L_2 periodic orbits, there are no dynamical structures such as invariant manifolds associated with periodic orbits around the triangular points in the Earth-Moon system. Therefore, transfer trajectories for direct asteroid capture can be designed from the candidate NEA's orbit to the short-period orbits around the Earth-Moon L_4/L_5 points directly, shown in Fig. 21(a). For the indirect capture strategy, we can patch the unstable manifolds of the Sun-Earth system with the short-period orbit around the Earth-Moon L_4/L_5 points, shown in Fig. 21(b).

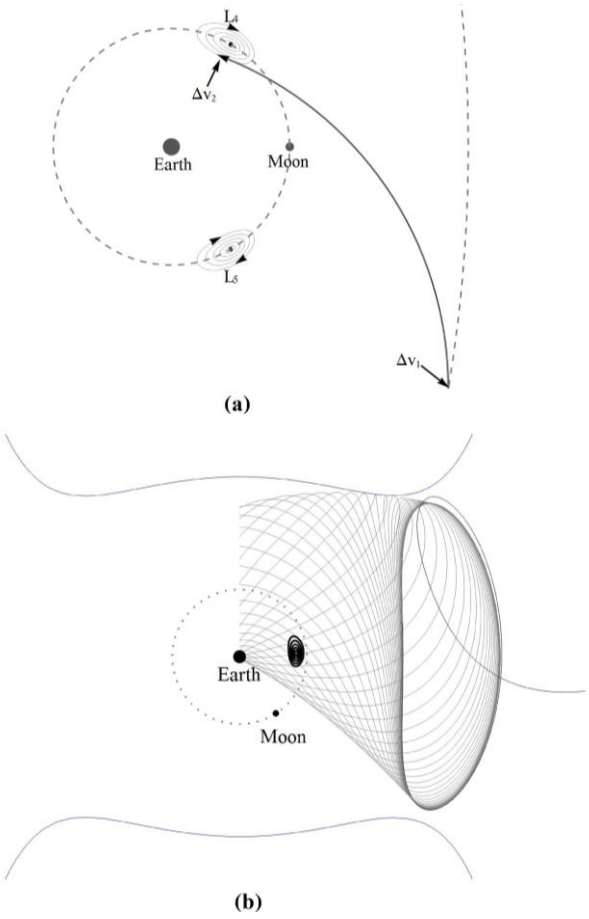

Fig. 21 Two types of asteroid capture strategies to the Earth-Moon triangular points: (a) direct capture; (b) indirect capture

Similar to the optimization of the direct/indirect capture trajectories to the Earth-Moon L_2 point, the direct/indirect capture trajectories to the Earth-Moon triangular points can again be optimized by using NSGA-II (Deb et al. 2002) followed by sequential quadratic programming (SQP) which is implemented in the function *fmincon* in MATLAB. The results of direct and indirect capture of asteroids to the triangular points in the Earth-Moon system is shown in Table 6 and Table 7. It can be seen that the direct asteroid capture method needs a shorter flight time, while the indirect asteroid capture method can achieve lower-cost asteroid capture. Compared to the results of Table 2 and Table 5, we can find that without invariant manifolds associated with the triangular points, it requires much more energy (i.e., Δv_2) to insert the candidate asteroids into the short-period orbits around the Earth-Moon triangular points. The optimal direct and indirect capture trajectories for 2014WX202 to the Earth-Moon triangular L_4 point is shown in Fig. 22. It should be noted that in the Table 7, 2L is short for the planar Lyapunov orbit around L_2.

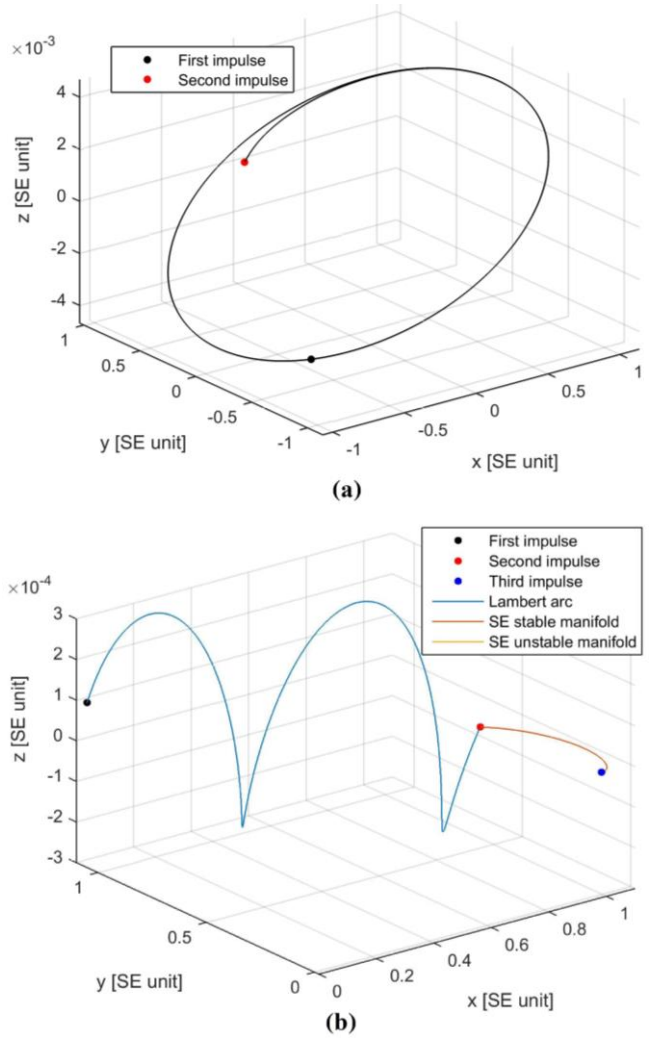

Fig. 22(a) Optimal direct capture trajectory for 2014WX202 to the Earth-Moon L_4 periodic orbit in the J2000 Sun-cantered inertial frame; (b) Optimal indirect capture trajectory for 2014WX202 to Earth-Moon L_4 periodic orbit in Sun-Earth rotating system

Table 6 Results of optimal direct capture of asteroids to the Earth-Moon triangular point

NEA	Δv_1 (ms^{-1})	Δv_2 (ms^{-1})	Δv (ms^{-1})	T_0 [MJD]	T_{fly} (day)	J_{EM}	Target (EM)
2014WX202	229.11	558.32	787.43	63300.0	646.3	2.97969193	L_4
2000SG344	310.72	412.11	722.83	61052.0	563.8	2.98187509	L_4
2010UE51	350.64	416.70	767.34	59445.1	440.0	2.97705019	L_4
2008EA9	90.14	756.81	846.96	58604.4	268.0	2.97489409	L_4
2007UN12	200.33	633.25	833.58	58840.7	260.7	2.97456372	L_4
2006RH120	348.20	378.24	726.44	61078.7	963.11	2.98147241	L_4

Table 7 Results of optimal indirect capture of asteroids to the Earth-Moon triangular point

NEA	$\Delta v_1+\Delta v_2$ (ms^{-1})	Δv_3 (ms^{-1})	Δv (ms^{-1})	T_0 [MJD]	T_{fly} (day)	J_{EM}	J_{SE}	Target (SE + EM)
2014WX202	407.55	179.84	587.39	62557.8	1579.1	2.89343059	3.00080537	2L+ L_4
2000SG344	494.48	188.82	683.3	60399.2	1367.0	2.97456372	3.00084945	2L+ L_4
2010UE51	370.00	289.00	658.98	58452.5	1984.6	2.98187510	3.00087784	2L+ L_4
2008EA9	539.21	248.60	787.80	58046.5	1362.3	2.97705020	3.00086915	2L+ L_4
2007UN12	316.30	237.24	553.54	58596.8	1058.6	2.97789448	3.00087056	2L+ L_4
2006RH120	349.35	195.73	545.08	60378.2	1836.7	2.97705020	3.00086915	2L+ L_4

Conclusion

The low-energy capture of near-Earth asteroids is of significant interest for both scientific and commercial purposes. It is a logical stepping stone towards more ambitious missions for space exploration in the future.

As a candidate gateway station, and an ideal location for interplanetary transfers, the Earth–Moon L_2 libration point is of great importance for future deep space exploration. Capturing asteroids and inserting them into periodic orbits around the Earth-Moon L_2 point offers in-situ resources to support such ventures. Therefore, the patched restricted three-body problem has been used to investigate the capture of asteroids into periodic orbits around the Earth-Moon L_2 point. However, using an indirect capture strategy via the Sun-Earth L_2 point the transfer duration is long due to the time required for the asteroid to move along the stable manifold in the Sun-Earth system.

Therefore, we propose a direct asteroid capture method to capture asteroids into periodic orbits around the Earth-Moon L_2 point from the asteroid's heliocentric orbit directly. An initial impulse is used to transfer the candidate asteroid to the appropriate stable manifold where it is then inserted directly onto the stable manifold in the Earth-Moon circular restricted three-body problem with a second impulse. Thus, the asteroid will be asymptotically captured onto a target periodic orbit around the L_2 point in Earth-Moon system. On the other hand, due to the stability of the triangular points in the CRTBP model, the vicinity of the triangular points in Earth-Moon system could be another preferred location for captured NEAs. The direct/indirect strategies are also applied to design the direct/indirect capture of asteroids to the triangular points. Since there are no invariant manifolds

associated with periodic orbits around the triangular points, transfer trajectories for direct asteroid capture can be designed from the candidate NEA's orbit to the short-period orbits around the Earth-Moon L_4/L_5 points directly and the indirect capture is designed by patching the unstable manifolds of the Sun-Earth system with the short-period orbit around the Earth-Moon L_4/L_5 points. Comparing the results of the two methods we find that the direct asteroid capture strategy requires a shorter flight time while the indirect asteroid capture strategy can always achieve a cheaper capture of NEAs in terms of energy requirements.

Acknowledgments

We acknowledge support through the China Scholarship Council (MT) and a Royal Society Wolfson Research Merit Award (CM).

References

Alessi, E.M., Gómez, G., Masdemont, J.J.: Leaving the Moon by means of invariant manifolds of libration point orbits. Communications in Nonlinear Science and Numerical Simulation **14**(12), 4153-4167 (2009)

Andrews, D.G., Bonner, K., Butterworth, A., Calvert, H., Dagang, B., Dimond, K., Eckenroth, L., Erickson, J., Gilbertson, B., Gompertz, N.: Defining a successful commercial asteroid mining program. Acta Astronautica **108**, 106-118 (2015)

Brophy, J., Culick, F., Friedman, L., Allen, C., Baughman, D., Bellerose, J., Betts, B., Brown, M., Busch, M., Casani, J.: Asteroid retrieval feasibility study. Keck Institute for Space Studies, Califonia Institute of Technology, Jet Propulsion Laboratory (2012a)

Brophy, J.R., Friedman, L., Culick, F.: Asteroid retrieval feasibility. In: Aerospace Conference, 2012 IEEE 2012b, pp. 1-16. IEEE

Ceriotti, M. and Sanchez, J.P.: Control of asteroid retrieval trajectories to libration point orbits. Acta Astronautica **126**, 342-353 (2016)

Davis, K.E., Anderson, R.L., Scheeres, D.J., Born, G.H.: The use of invariant manifolds for transfers between unstable periodic orbits of different energies. Celestial Mechanics and Dynamical Astronomy **107**(4), 471-485 (2010)

Davis, K.E., Anderson, R.L., Scheeres, D.J., Born, G.H.: Optimal transfers between unstable periodic orbits using invariant manifolds. Celestial Mechanics and Dynamical Astronomy **109**(3), 241-264 (2011)

de Sousa-Silva, P.A. and Terra, M.O.: A survey of different classes of Earth-to-Moon trajectories in the patched three-body approach. Acta Astronautica **123**, 340-349 (2016)

Deb, K., Pratap, A., Agarwal, S., Meyarivan, T.: A fast and elitist multiobjective genetic algorithm: NSGA-II. IEEE transactions on evolutionary computation **6**(2), 182-197 (2002)
DeFilippi Jr, G.: Station keeping at the L4 libration point: A three dimensional study. AIR FORCE INST OF TECH WRIGHT-PATTERSON AFB OH SCHOOL OF ENGINEERING (1977)
Farquhar, R.W., Dunham, D.W., Guo, Y., McAdams, J.V.: Utilization of libration points for human exploration in the Sun–Earth–Moon system and beyond. Acta Astronautica **55**(3), 687-700 (2004)
Folta, D., Woodard, M., Cosgrove, D.: Stationkeeping of the First Earth-Moon Libration Orbiters: The ARTEMIS Mission. In: AAS 11-515, Proceedings of the AAS/AIAA Astrodynamics Specialist Conference, Girdwood, Alaska 2011
Gómez, G.: Dynamics and Mission Design Near Libration Points, Vol I: Fundamentals: the Case of Collinear Libration Points, vol. 1. World Scientific, Singapore (2001)
Gómez, G., Jorba, A., Masdemont, J., Simó, C.: Study refinement of semi-analytical halo orbit theory. Final Report, ESOC Contract(8625/89) (1991)
Gao, Y.: Near-Earth asteroid flyby trajectories from the Sun-Earth L2 for Chang'e-2's extended flight. Acta Mechanica Sinica **29**(1), 123-131 (2013)
Hasnain, Z., Lamb, C.A., Ross, S.D.: Capturing near-Earth asteroids around Earth. Acta Astronautica **81**(2), 523-531 (2012)
Howell, K. and Pernicka, H.: Numerical determination of Lissajous trajectories in the restricted three-body problem. Celestial Mechanics **41**(1-4), 107-124 (1987)
Howell, K.C. and Kakoi, M.: Transfers between the Earth–Moon and Sun–Earth systems using manifolds and transit orbits. Acta Astronautica **59**(1), 367-380 (2006)
Hufenbach, B., Laurini, K., Piedboeuf, J., Schade, B., Matsumoto, K., Spiero, F., Lorenzoni, A.: The Global Exploration Roadmap. In: IAC-11-B3.1.8, 62nd International Astronautical Congress, Capetown, SA 2011
Koon, W., Lo, M., Marsden, J., Ross, S.: Low Energy Transfer to the Moon. Celestial Mechanics and Dynamical Astronomy **81**(1-2), 63-73 (2001)
Koon, W.S., Lo, M.W., Marsden, J.E., Ross, S.D.: Shoot the moon. Spaceflight Mechanics 2000, Vol 105, Pts I and Ii **105**, 1017-1030 (2000)
Koon, W.S., Lo, M.W., Marsden, J.E., Ross, S.D.: Dynamical systems, the three-body problem and space mission design. Springer-Verlag, New York (2011)
Lo, M. and Ross, S.: The Lunar L1 Gateway: Portal to the stars and beyond. In: A01-40254, AIAA Space 2001 Conference and Exposition, Albuquerque, NM, U.S.A 2001
Lo, M.W. and Parker, J.S.: Unstable resonant orbits near earth and their applications in planetary missions. In: AIAA 2004-5304, AIAA/AAS Astrodynamics Specialist Conference, vol. 2004-5304. Providence, RI, (2004)
Mingotti, G., Sánchez, J., McInnes, C.: Combined low-thrust propulsion and invariant manifold trajectories to capture NEOs in the Sun–Earth circular restricted three-body problem. Celestial Mechanics and Dynamical Astronomy **120**(3), 309-336 (2014a)

Mingotti, G., Sanchez, J.-P., McInnes, C.: Low energy, low-thrust capture of near Earth objects in the Sun–Earth and Earth–Moon restricted three-body systems. In: AIAA 2014-4301, SPACE Conferences & Exposition. AIAA, Washington 2014b

O'Neill, G.: The Colonization of Space. Physics Today **27(9)**, 32-40 (1974)

Olson, J.: Voyages: charting the course for sustainable human space exploration. In: National Aeronautics and Space Administration. NASA, (2012)

Qi, Y. and Xu, S.: Study of lunar gravity assist orbits in the restricted four-body problem. Celestial Mechanics and Dynamical Astronomy, 1-29 (2016)

Richardson, D.L.: Analytic construction of periodic orbits about the collinear points. Celestial mechanics **22**(3), 241-253 (1980)

Sánchez, J.P. and Yárnoz, D.G.: Asteroid retrieval missions enabled by invariant manifold dynamics. Acta Astronautica **127**, 667-677 (2016)

Salazar, F., de Melo, C., Macau, E., Winter, O.: Three-body problem, its Lagrangian points and how to exploit them using an alternative transfer to L4 and L5. Celestial Mechanics and Dynamical Astronomy **114**(1-2), 201-213 (2012)

Sanchez, J.-P., Garcia Yarnoz, D., Alessi, E.M., McInnes, C.: Gravitational capture opportunites for asteroid retrieval missions. In: IAC-12.C1.5.13x14763, 63rd International Astronautical Congress, Naples, Italy 2012

Sanchez, J.P. and McInnes, C.R.: On the ballistic capture of asteroids for resource utilisation. In: IAC-11.C1.4.6, 62nd International Astronautical Congress, CapeTown, SA 2011

Szebehely, V.: Theory of orbit: The restricted problem of three Bodies. Elsevier, (1967)

Topputo, F.: On optimal two-impulse Earth–Moon transfers in a four-body model. Celestial Mechanics and Dynamical Astronomy **117**(3), 279-313 (2013)

Tronchetti, F.: Private property rights on asteroid resources: Assessing the legality of the ASTEROIDS Act. Space Policy **30**(4), 193-196 (2014)

Wang, Y.M., Qiao, D., Cui, P.Y.: Trajectory Design for the Transfer from the Lissajous Orbit of Sun-Earth System to Asteroids. Applied Mechanics and Materials **390**, 478-484 (2013)

Yárnoz, D.G., Sanchez, J., McInnes, C.: Easily retrievable objects among the NEO population. Celestial Mechanics and Dynamical Astronomy **116**(4), 367-388 (2013)

Zhang, Z. and Hou, X.: Transfer orbits to the Earth–Moon triangular libration points. Advances in Space Research **55**(12), 2899-2913 (2015)

Zimmer, A.: Investigation of vehicle reusability for human exploration of Near-Earth Asteroids using Sun–Earth Libration point orbits. Acta Astronautica **90**(1), 119-128 (2013)